



OPEN ACCESS

EDITED BY
Daniel Abate-Daga,
Moffitt Cancer Center, United States

REVIEWED BY
Nelli Bejanyan,
Moffitt Cancer Center, United States
Jeffrey A. Medin,
Medical College of Wisconsin,
United States

*CORRESPONDENCE
H. Trent Spencer
✉ hspence@emory.edu

RECEIVED 14 September 2023
ACCEPTED 26 October 2023
PUBLISHED 13 November 2023

CITATION

Branella GM, Lee JY,
Okalova J, Parwani KK, Alexander JS,
Arthuzo RF, Fedanov A, Yu B, McCarty D,
Brown HC, Chandrakasan S, Petrich BG,
Doering CB and Spencer HT (2023)
Ligand-based targeting of c-kit using
engineered $\gamma\delta$ T cells as a strategy for
treating acute myeloid leukemia.
Front. Immunol. 14:1294555.
doi: 10.3389/fimmu.2023.1294555

COPYRIGHT

© 2023 Branella, Lee, Okalova, Parwani,
Alexander, Arthuzo, Fedanov, Yu, McCarty,
Brown, Chandrakasan, Petrich, Doering and
Spencer. This is an open-access article
distributed under the terms of the [Creative Commons Attribution License \(CC BY\)](https://creativecommons.org/licenses/by/4.0/). The
use, distribution or reproduction in other
forums is permitted, provided the original
author(s) and the copyright owner(s) are
credited and that the original publication in
this journal is cited, in accordance with
accepted academic practice. No use,
distribution or reproduction is permitted
which does not comply with these terms.

Ligand-based targeting of c-kit using engineered $\gamma\delta$ T cells as a strategy for treating acute myeloid leukemia

Gianna M. Branella^{1,2,3}, Jasmine Y. Lee^{1,2,3}, Jennifer Okalova^{1,3,4},
Kiran K. Parwani^{1,2,3}, Jordan S. Alexander^{1,3},
Raquel F. Arthuzo^{1,2,3}, Andrew Fedanov^{1,3}, Bing Yu⁵,
David McCarty⁵, Harrison C. Brown⁵,
Shanmuganathan Chandrakasan^{1,3}, Brian G. Petrich⁵,
Christopher B. Doering^{1,3,4} and H. Trent Spencer^{1,3,4*}

¹Department of Pediatrics, Emory University School of Medicine, Atlanta, GA, United States, ²Graduate Division of Biological and Biomedical Sciences, Laney Graduate School, Emory University, Atlanta, GA, United States, ³Aflac Cancer and Blood Disorders Center, Children's Healthcare of Atlanta, Atlanta, GA, United States, ⁴Molecular Systems Pharmacology Program, Graduate Division of Biological and Biomedical Sciences, Laney Graduate School, Emory University, Atlanta, GA, United States, ⁵Expression Therapeutics, Inc., Tucker, GA, United States

The application of immunotherapies such as chimeric antigen receptor (CAR) T therapy or bi-specific T cell engager (BiTE) therapy to manage myeloid malignancies has proven more challenging than for B-cell malignancies. This is attributed to a shortage of leukemia-specific cell-surface antigens that distinguish healthy from malignant myeloid populations, and the inability to manage myeloid depletion unlike B-cell aplasia. Therefore, the development of targeted therapeutics for myeloid malignancies, such as acute myeloid leukemia (AML), requires new approaches. Herein, we developed a ligand-based CAR and secreted bi-specific T cell engager (sBite) to target c-kit using its cognate ligand, stem cell factor (SCF). c-kit is highly expressed on AML blasts and correlates with resistance to chemotherapy and poor prognosis, making it an ideal candidate for which to develop targeted therapeutics. We utilize $\gamma\delta$ T cells as a cytotoxic alternative to $\alpha\beta$ T cells and a transient transfection system as both a safety precaution and switch to remove alloreactive modified cells that may hinder successful transplant. Additionally, the use of $\gamma\delta$ T cells permits its use as an allogeneic, off-the-shelf therapeutic. To this end, we show mSCF CAR- and hSCF sBite-modified $\gamma\delta$ T cells are proficient in killing c-kit⁺ AML cell lines and sca-1⁺ murine bone marrow cells *in vitro*. *In vivo*, hSCF sBite-modified $\gamma\delta$ T cells moderately extend survival of NSG mice engrafted with disseminated AML, but therapeutic efficacy is limited by lack of $\gamma\delta$ T-cell homing to murine bone marrow. Together, these data demonstrate preclinical efficacy and support further investigation of SCF-based $\gamma\delta$ T-cell therapeutics for the treatment of myeloid malignancies.

KEYWORDS

acute myeloid leukemia (AML), gamma delta ($\gamma\delta$) T cells, ligand-based therapeutics, chimeric antigen receptor (CAR), secreted bispecific T cell engager, stem cell factor (SCF), c-kit (CD117)

1 Introduction

Adoptive cell therapy (ACT), such as chimeric antigen receptor (CAR) T therapy, has significantly advanced the treatment of B cell malignancies, leading to the FDA approval of multiple cellular products (1–6). However, ACT for other leukemias, like acute myeloid leukemia (AML), do not share the same success. Current treatment regimens for AML consist of genotoxic chemotherapeutics (7) that have severe toxicities in the bone marrow (8), with approximately 30% of children relapsing (9–12). This leads to a drop in survival from 70% to a mere 20% (9, 13), highlighting the need for new treatment options.

Unfortunately, there are a lack of known leukemia-specific, cell-surface antigens that distinguish healthy from malignant myeloid cells (14). This makes the translation of traditional cell-based immunotherapies with long-term persistence challenging in this setting, as myeloid depletion cannot be managed like B-cell aplasia. However, as hematopoietic stem cell transplantation (HSCT) is considered curative for AML, it may be important to take advantage of novel therapeutics that display off-tumor toxicities in the hematopoietic compartment that can be corrected with HSCT. In fact, toxicity within the bone marrow may prove advantageous to dually prepare the patient for transplant and target residual disease congruently.

We have developed receptor-directed, ligand-based ACT to target malignant myeloid tissue through interaction with c-kit using its cognate ligand, stem cell factor (SCF). Up to 90% of AML patients have c-kit expression correlating with poor prognosis and resistance to chemotherapy (15, 16), making this receptor an attractive target for malignant myeloid cell and leukemic stem cell (LSC) ablation. In fact, we (17) and others (18–22) have shown the continued use of c-kit as a target for non-genotoxic conditioning due to its expression on hematopoietic stem cells (HSCs). These therapies have proven safe for use in preclinical murine models with toxicities only observed within the hematopoietic compartment (17) despite limited c-kit expression on some organs outside of the hematopoietic compartment, like the cerebellum, female reproductive organs, and lungs. Clinically, c-kit is the target of monoclonal antibody briquilimab, which has shown promise in treating patients with AML and myelodysplastic syndromes (MDS) in a Phase 1 clinical trial (NCT04429191), Fanconi anemia in a Phase 1/2 clinical trial (NCT04784052), severe combined immunodeficiency (SCID) in a Phase 1/2 clinical trial (NCT02963064), and sickle cell disease in a Phase 1/2 clinical trial (NCT05357482) with no treatment-related adverse events in 130 dosed subjects as of late September 2023 (23, 24).

Herein, we utilize ligand-based, c-kit-directed, CAR- and secreted bispecific T-cell engager (sBite)-modified T cells as a therapeutic for the treatment of AML. Traditionally, CARs and bispecific antibodies are designed with single chain variable fragments (scFvs) as their antigen-binding domains that specifically redirect T cells to kill cancer cells without the need for antigen processing and presentation by the human leukocyte antigen (HLA) (25). However, these designs are not without flaws. Primarily, scFv molecules are prone to aggregation and produce higher order complexes through intermolecular variable

heavy (V_H) and variable light (V_L) association, resulting in tonic signaling and thereby lower therapeutic efficacy (26–28). Our proposed ligand-based design circumvents these issues.

Furthermore, we employ CAR- and sBite-modified $\gamma\delta$ T cells as a cytotoxic alternative to $\alpha\beta$ T cells. $\gamma\delta$ T cells contribute to graft-versus-leukemia (GvL) reactions to enhance cancer eradication through the recognition of stress antigens expressed by leukemia cells (29–31). Additionally, as $\gamma\delta$ T cells recognize antigen independent of HLA, they can be transplanted across HLA barriers in the presence of immunosuppression, thus creating opportunity for an off-the-shelf therapeutic. Importantly, we (31–36) and others (37) have optimized the use of $\gamma\delta$ T cells and can expand these cells *ex vivo* using a novel serum-free protocol resulting in a cellular product of highly purified $V\gamma9V\delta2$ T cells with low percentages of NK cells and negligible $\alpha\beta$ T cell contamination. The chemokine receptor expression and exhaustion profiles of these cells have been reported (35, 38), in addition to the phenotype of the contaminating NK cells within our cellular product (38).

These studies establish a ligand-based cell therapy strategy using engineered $\gamma\delta$ T cells as a cytotoxic alternative to traditional ACT for the treatment of AML. Non-modified allogeneic $\gamma\delta$ T cells expanded under our Good Manufacturing Practice (GMP)-compliant serum-free protocol are currently under clinical investigation in a Phase 1 trial for the treatment of relapsed/refractory neuroblastoma (NCT05400603). In the context of myeloid malignancies, we have previously demonstrated non-modified $\gamma\delta$ T cells have enhanced cytotoxicity against AML cell lines in combination with chemotherapeutic agents that upregulate stress antigens expressed by AML cells (31). More recently, we showed our efforts in optimizing and utilizing expanded $\gamma\delta$ T cells transiently transfected with mRNA encoding a CD19 CAR for the treatment of B-cell malignancies (39). Here, we expand our repertoire by investigating the transient modification of $\gamma\delta$ T cells using a ligand-based CAR and sBite. These studies provide the basis for further investigation into the use of ligand-based $\gamma\delta$ T cell therapies.

2 Materials and methods

2.1 c-kit and NKG2D ligand expression on healthy donor and patient samples

The St. Jude Cloud (pecan.stjude.cloud) was queried for c-kit expression using transcriptomic data from 2,480 pediatric patients (40, 41). The Human Protein Atlas (v22.proteinatlas.org) was queried for c-kit expression in healthy tissues and cell lines by RNA sequencing (42). The R2 Genomics Analysis and Visualization Platform (<https://r2.amc.nl>) was used to query multiple datasets using the Megasampler R2 module for expression of c-kit, ULBP1, ULBP2, and MICA/MICB by RNA sequencing. The u133a chip with MAS5.0 normalization was used exclusively. Datasets utilized in this study were as follows: PBMC (Novershtern, 211 samples), HSC (OGIC, 21 samples), and AML (Bohlander, 422 samples and Delwel, 293 samples).

2.2 Cell lines

The NOMO-1, Kasumi-1, KG-1, and MOLM-13 cell lines were kindly gifted by the laboratory of Dr. Douglas Graham (Emory University, Atlanta, GA, USA). The CMK cell line was kindly provided by the laboratory of Dr. Brian Petrich (Emory University, Atlanta, GA, USA). The Jurkat, K562, and 697 cell lines were obtained from the American Type Culture Collection (Manassas, VA, USA). NOMO-1, K562, 697, KG-1, and Jurkat cells were cultured in RPMI-1640 with L-glutamine (Corning CellGro, Manassas, VA, USA) supplemented with 10% fetal bovine serum (FBS; R&D Systems, Minneapolis, MN, USA) and 1% Penicillin-Streptomycin (Cytiva, Marlborough, MA, USA). The CMK, Kasumi-1, and MOLM-13 cell lines were cultured under the same conditions using 20% FBS.

2.3 Design and cloning of mSCF CAR and hSCF sBite

mSCF CAR and hSCF sBite DNA sequences were cloned into vectors containing the necessary components for mRNA or lentiviral production as follows:

To clone the mSCF CAR, the full-length DNA sequence for secreted murine SCF obtained from UniProt (uniprot.org) (43) was ordered as a gene fragment product flanked by AscI and NheI restriction enzyme sites or BamHI and NotI restriction enzyme sites (Integrated DNA Technologies, Coralville, IA, USA). The gene fragment product was cloned into a recipient plasmid with paired AscI and NheI or BamHI and NotI sites upstream of the CD8 α , CD28, and CD3 ζ CAR components using corresponding restriction enzymes AscI and NheI or BamHI and NotI (New England BioLabs, Ipswich, MA, USA) behind a UBC or T7 promoter. The DNA construct was codon optimized for expression in T cells by Expression Therapeutics (Tucker, GA, USA) using Expression Cassette Optimization (eCO) technology and confirmed by Sanger sequencing (Genewiz, Burlington, MA, USA).

To clone the hSCF sBite, the coding sequence of secreted isoform of human SCF was obtained from GenBank (M59964.1). The sequence of the SCF signal peptide through mature core fragment was identified as bases 1- 426 of the native cDNA sequence. To generate the sBite, this fragment was combined with a G4S linker and CD3 scFv derived from clone OKT3. The sequence was then codon optimized for expression in $\gamma\delta$ T cells by Expression Therapeutics (Tucker, GA, USA) using Expression Cassette Optimization (eCO) technology. The optimized sequence was then synthesized and cloned into a pcDNA3.1-based plasmid using seamless ligation technology by Genscript (Piscataway, NJ, USA) behind a T7 promoter.

2.4 Production of mSCF CAR and hSCF sBite mRNA

The mMessage mMachine T7 Transcription kit (Thermo Fisher Scientific, Waltham, MA, USA) was used to produce mSCF CAR

mRNA after linearization with restriction enzyme XhoI, whose restriction site cuts directly after the CD3 ζ sequence.

The HiScribe T7 mRNA kit with CleanCap Reagent AG Plasmid (New England BioLabs, Ipswich, MA, USA) was used to produce hSCF sBite Cap-1 mRNA after linearization with NotI. Poly(a) tailing was subsequently performed using E. coli poly(a) polymerase (New England BioLabs, Ipswich, MA, USA).

RNA gel electrophoresis was used to confirm efficient poly-A tail extension and quality of mRNA products.

2.5 Production of mSCF CAR and CD19 CAR lentiviral vectors

High-titer, recombinant, self-inactivating HIV lentiviral vectors were produced and titered as previously described (44–46). Briefly, HEK-293T cells were transiently transfected with packaging plasmids encoding Gag-Pol, Rev, VSVG envelope, and the CAR transgene plasmid using calcium phosphate (Sigma Aldrich, St. Louis, MO, USA). Cells were cultured in DMEM (Thermo Fisher Scientific, Waltham, MA, USA) supplemented with 10% FBS and supernatant was collected for 3 days beginning 48 hours after transfection. Supernatants were passed through a 0.45- μ m filter, pooled, and concentrated by overnight centrifugation at 10,000 \times g at 4°C. The following morning, viral particles were passed through a 0.22- μ m filter and stored at -80°C. Titers were determined using quantitative real-time PCR analysis on HEK-293T cell genomic DNA.

2.6 Expansion and modification of primary $\alpha\beta$ T cells

Peripheral blood from healthy adult volunteers were obtained under an IRB approved protocol (IRB00101797) through the Emory University Children's Clinical and Translational Discovery Core (CCTDC), after which peripheral blood mononuclear cells (PBMCs) were isolated using a Ficoll-Plaque PLUS density gradient (GE HealthCare, Chicago, IL, USA) and cryopreserved. Alternatively, cryopreserved PBMCs were procured from AllCells (Alameda, CA, USA). T cells were negatively selected from thawed PBMCs using the EasySep Human T cell Isolation Kit (Stemcell Technologies, Vancouver, BC, CA) and stimulated with anti-CD3/CD28 Human T-Activator Dynabeads (Thermo Fisher Scientific, Waltham, MA, USA) at a 1:1 bead-to-cell ratio in X-VIVO 15 (Lonza, Basel, Switzerland) supplemented with 10% FBS, 1% penicillin-streptomycin, 100 IU/mL human IL-2 (PeproTech, Rocky Hill, NJ, USA), and 5 ng/mL human IL-7 (PeproTech, Rocky Hill, NJ, USA) at 2×10^6 cells/mL. After 48 hours of stimulation, beads were removed and 1×10^6 cells were transduced at MOI 20 with 10 μ g/mL polybrene (EMD Millipore, Billerica, MA, USA) for 18 hours. MOI was determined using the following calculation:

$$\text{MOI} = \frac{\text{titer} \times \text{volume (mL)}}{\# \text{ of cells}}$$

After 18 hours, cells were resuspended in fresh media and underwent an early cell dilution of ~100,000 cells/mL, then left to expand for 96 hours before CAR expression was determined and used in cytotoxicity assays or animal studies.

2.7 Expansion and transfection of primary $\gamma\delta$ T cells

Peripheral blood from healthy consenting volunteers (30–40 mL) was obtained as previously mentioned (under the Expansion and modification of primary $\alpha\beta$ T cells section) through the CCTDC or fresh leukopaks were procured from the American Red Cross. From either source, PBMCs were isolated using a Ficoll-Plaque PLUS density gradient and cultured in OpTmizer serum-free media (Thermo Fisher Scientific, Waltham, MA, USA) supplemented with 2 mM L-glutamine, 1% penicillin-streptomycin, 500–1000 IU/mL human IL-2, and 5 μ M zoledronic acid (Sigma-Aldrich, St. Louis, MO, USA) using our previously published Good Manufacturing Practice-compliant 12-day expansion protocol (31, 33, 35). Expanded $\gamma\delta$ T cells were cryopreserved in 5% human serum albumin (HSA; Grifols, Barcelona, Spain) and 10% dimethylsulfoxide (DMSO; Sigma-Aldrich, St. Louis, MO, USA) diluted in PlasmaLyte A (Baxter International Inc. Deerfield, IL, USA) in 1×10^7 – 1×10^8 cell aliquots.

Cryopreserved $\gamma\delta$ T cells were thawed in three volumes of 5% HSA diluted in PlasmaLyte A and centrifuged at $250 \times g$ for 10 minutes. Cells were resuspended in OpTmizer serum-free media supplemented with 2 mM L-glutamine, 1% penicillin-streptomycin, and 1000 IU/mL of human IL-2 and rested for 2 hours at 37°C, 5% CO₂. Rested $\gamma\delta$ T cells (5 – 25×10^6 cells) were then transiently transfected to express an mSCF CAR or hSCF sBite through mRNA electroporation by first washing the cells three times with PBS and spinning at $250 \times g$ for 10 minutes, then resuspending in Opti-MEM (ThermoFisher Scientific, Waltham, MA, USA) with 15 μ g of purified mRNA or equal volume vehicle control for mock transfection. Cells were then electroporated using a square wave function at 500 V for 5 ms in a 4 mm electroporation cuvette (Fisher Scientific, Hampton, NH, USA) using the GenePulser Xcell Electroporation System (Bio-Rad Laboratories, Hercules, CA, USA). Modified $\gamma\delta$ T cells were used 24 hours after electroporation for *in vitro* studies and 1–4 hours after electroporation for *in vivo* studies.

2.8 Measuring CAR expression by western blotting

mSCF CAR-modified cells were lysed with RIPA buffer (Sigma-Aldrich, St. Louis, MO, USA) supplemented with Protease Inhibitor Cocktail diluted 1:100 (Sigma-Aldrich, St. Louis, MO, USA) and PMSF protease inhibitor diluted 1:100 (ThermoFisher Scientific, Waltham, MA, USA) for 30 minutes on ice, after which cell lysates were clarified by centrifugation at $14,000 \times g$ at 4°C for 10 minutes. The supernatant was collected as a whole cell lysate. Protein

concentrate was quantified using a Bradford Assay (Bio-Rad Laboratories, Hercules, CA, USA). 20–40 μ g of protein was first heated at 100°C for 10 minutes, then loaded into a 4–15% pre-cast gel (Bio-Rad Laboratories, Hercules, CA, USA) with Precision Plus Protein Dual Color Standards (Bio-Rad Laboratories, Hercules, CA, USA) and separated by SDS-PAGE. Protein was transferred to a nitrocellulose membrane (Bio-Rad Laboratories, Hercules, CA, USA) at 250 constant Amps for 60 minutes and then washed in TBS containing 0.1% Tween-20 prior to incubation with a mouse anti-human CD3 ζ primary antibody diluted 1:1000 (BioLegend, San Diego, CA, USA) and goat anti-mouse HRP secondary antibody diluted 1:500 (BioLegend, San Diego, CA, USA). Blots were then imaged by chemiluminescence with a Bio-Rad ChemiDoc XR+ Molecular Imager.

2.9 Measuring CAR expression by flow cytometry

Jurkat or primary CAR T cells were stained with 20 ng of Recombinant Mouse c-kit Fc Chimera Protein (R&D Systems, Minneapolis, MN, USA) or 20 ng of Recombinant Human c-kit Fc Chimera Protein (R&D Systems, Minneapolis, MN, USA) and incubated on ice for 30 minutes. Cells were washed once with FACS buffer (PBS + 2.5% FBS), then stained with 2 μ L R-Phycoerythrin F (ab')₂ secondary antibody (Jackson ImmunoResearch, West Grove, PA, USA) and eBioscience Fixable Viability Dye eFluor 780 (Thermo Fisher Scientific, Waltham, MA, USA) to exclude dead cells and incubated on ice for 15 minutes. Cells were then washed once with FACS buffer, then subjected to flow cytometry (Cytek Aurora) and analyzed with FlowJo software (v10).

2.10 *In vitro* cytotoxicity assays

To assess the cytotoxicity of mSCF CAR- or hSCF sBite-T cells against AML cell lines, unmodified or modified primary T cells were co-cultured with 50,000 target cells (CMK or Kasumi-1) stained with VPD450 (BD, Franklin Lakes, NJ, USA) at indicated effector-to-target ratios for 4–24 hours at 37°C, 5% CO₂. Co-cultures were then washed once with Annexin V Binding Buffer (0.025 mM calcium chloride + 1.4 mM sodium chloride + 0.1 mM HEPES) and stained with 3 μ L Annexin V-APC (BioLegend, San Diego, CA, USA) for 20 minutes at room temperature. Cells were then washed once with Annexin V Binding Buffer. 7-AAD Viability Dye (BioLegend, San Diego, CA, USA) was added 2 minutes before the sample was subjected to flow cytometric analysis (Cytek Aurora). Samples were analyzed with FlowJo software (v10), where percent cytotoxicity was measured by the sum of Annexin V⁺, 7-AAD⁺, and Annexin-V⁺/7-AAD⁺ target cells.

2.11 *In vitro* activation assays

Jurkat or primary CAR T cells were co-cultured with VPD450 (BD, Franklin Lakes, NJ, USA) stained target cells (CMK, Kasumi-1,

Nomo-1, or 697) at indicated effector-to-target ratios for 4 hours at 37°C, 5% CO₂. Co-cultures were then washed once with FACS buffer and stained with 3 µL anti-CD69-APC-Cy7 antibody (BD, Franklin Lakes, NJ, USA) for 20 minutes at 4°C. After staining, cells were washed once with FACS buffer, then subjected to flow cytometry (Cytek Aurora) and analyzed with FlowJo software (v10). Dead cells were excluded from the analysis using 3 µL of 7-AAD Viability Dye added 2 minutes before analysis on the cytometer.

2.12 Colony forming unit assay

For each bone marrow sample, 0.8–8 × 10⁴ cells isolated from mouse femurs by flushing were first resuspended in RPMI 1640 supplemented with 10% FBS and 1% penicillin-streptomycin. Resuspended cells were then added to 4 mL Methocult GF M3434 (Stemcell Technologies, Vancouver, BC, CA) and plated on sterile 35 mm plates in triplicate. Plates were incubated at 37°C 5% CO₂ for 7 days, then colonies were counted under a microscope.

2.13 Animal studies

NOD.Cg-Prkdc^{scid}Il2rg^{tw1Wj}/SzJ (NSG) mice were purchased from Jackson Laboratories (Bar Harbor, ME, USA) and maintained in a pathogen-free environment at an Emory University Division of Animal Resources facility. All animal studies were conducted in accordance with established policies set forth by the Emory University Institutional Animal Care and Use Committee (IACUC) under an approved animal use protocol (PROTO201800202). Equal numbers of male and female mice were used for all studies.

To determine the toxicity of mSCF CAR-modified αβ T cells, 8-week-old NSG mice were first preconditioned with 100 rads of x-ray irradiation (Rad Source Technologies, RS 2000 Small Animal Irradiator, Buford, GA, USA) then administered 5 × 10⁶ luciferase-modified CMK cells by intravenous injection into the lateral tail-vein the following morning. The following day, mice were either treated with 5 × 10⁶ mock-transduced αβ T cells (n = 6) or mSCF CAR-modified αβ T cells (n = 6, transduction efficiency < 8%) via tail-vein injection, with PBS administered as an untreated control (n = 3). Peripheral blood was collected at 3 weeks to assess for tumor burden and CAR T-cell engraftment. Mice were euthanized when end-point criteria were met, which includes changes in weight, scruff, movement, and hunched state.

To examine the persistence of γδ T cells in mice, 7–13-week-old NSG mice were administered 1 × 10⁷ non-modified γδ T cells via retro-orbital injection. In an effort to enhance persistence, mice were either treated with vehicle control (n = 6), 13,000 IU IL-2 twice a week via intraperitoneal injection (n = 6), or a combination of 13,000 IU IL-2 twice a week via intraperitoneal injection and 70 µg/kg zoledronic acid (NorthStar Rx, Memphis, TN, USA) via subcutaneous injection (n = 6). Once a day for 4 days, peripheral blood was collected, and leukocytes were assessed for the presence of human CD45⁺ cells by flow cytometric analysis (Cytek Aurora) and analyzed with FlowJo software (v10). On day 4, mice were euthanized, and spleens and bone marrow were harvested to assess for the presence of human CD45⁺ cells as before.

To examine the toxicity of mSCF CAR-modified γδ T cells in mice, 8–12-week-old NSG mice were anesthetized and administered 2–8 × 10⁶ mock transfected γδ T cells (n = 4) or mSCF CAR-modified γδ T cells (n = 4), with PBS as an untreated control (n = 3) via intraosseous injection in the left femur. Mice were given 5 mg/kg meloxicam (Baudax Bio, Malvern, PA, USA) via subcutaneous injection immediately after the intraosseous injection as an analgesic. After 2 days, mice were euthanized and peripheral blood, spleens, and bone marrow from both the left and the right femur were harvested to assess for the presence of human CD3⁺ human γδTCR⁺ cells and murine c-kit⁺ cells by flow cytometry (Cytek Aurora). Data was analyzed using the FlowJo software (v10). At this time, a CFU assay was performed to assess for multipotent progenitor cells. The left and the right femurs from each mouse were kept as separate samples in the flow and CFU assays in this experiment.

To assess the cytotoxicity of mSCF CAR- and hSCF sBite-modified γδ T cells in an AML model, 5–9-week-old NSG mice were first preconditioned with 20 mg/kg busulfan (DSM Pharmaceuticals, Inc., Greenville, NC, USA) via intraperitoneal injection, then administered 5 × 10⁶ luciferase-modified CMK cells via tail-vein injection the following morning. Beginning in the afternoon on the same day and then once daily for the following 3 days for a total of 4 doses, mice were treated with 1 × 10⁷ mock transfected γδ T cells (n = 6), mSCF CAR-modified γδ T cells (n = 3), or hSCF sBite-modified γδ T cells (n = 6) by intravenous injection into the lateral tail-vein, with PBS to serve as an untreated control (n = 8). Tumor growth and overall health of the mice were monitored two times per week IVIS (*In vivo* Imaging System, Perkin Elmer, Waltham, MA, USA) imaging and weighing, respectively. Freshly made D-luciferin (PerkinElmer, Waltham, MA, USA) was injected at 150 mg/kg via intraperitoneal injection 10 minutes prior to imaging. Bioluminescence was quantified using Living Image Software (PerkinElmer, Waltham, MA, USA) or Aura Software (Spectral Instruments Imaging, Tucson, AZ, USA). Peripheral blood was collected at 3 weeks to assess for c-kit expression on CD33⁺ AML cells and to perform complete blood counts. Mice were euthanized when end-point criteria were met, which includes changes in weight, scruff, movement, and hunched state.

2.14 Statistical analysis

All statistical analyses were performed using Prism 8 software (GraphPad Software Inc). Results are presented as mean ± standard deviation of the mean and were considered statistically significant at *P* < 0.05. Unpaired or paired two-tailed Student's *t*-test, one-way ANOVA, or log-rank (Mantel-Cox) test were used to determine statistical significance as appropriate.

3 Results

3.1 c-kit is highly expressed on pediatric AML and healthy HSCs

We first sought to determine c-kit expression on healthy tissues. The Human Protein Atlas (proteintlas.org) demonstrates

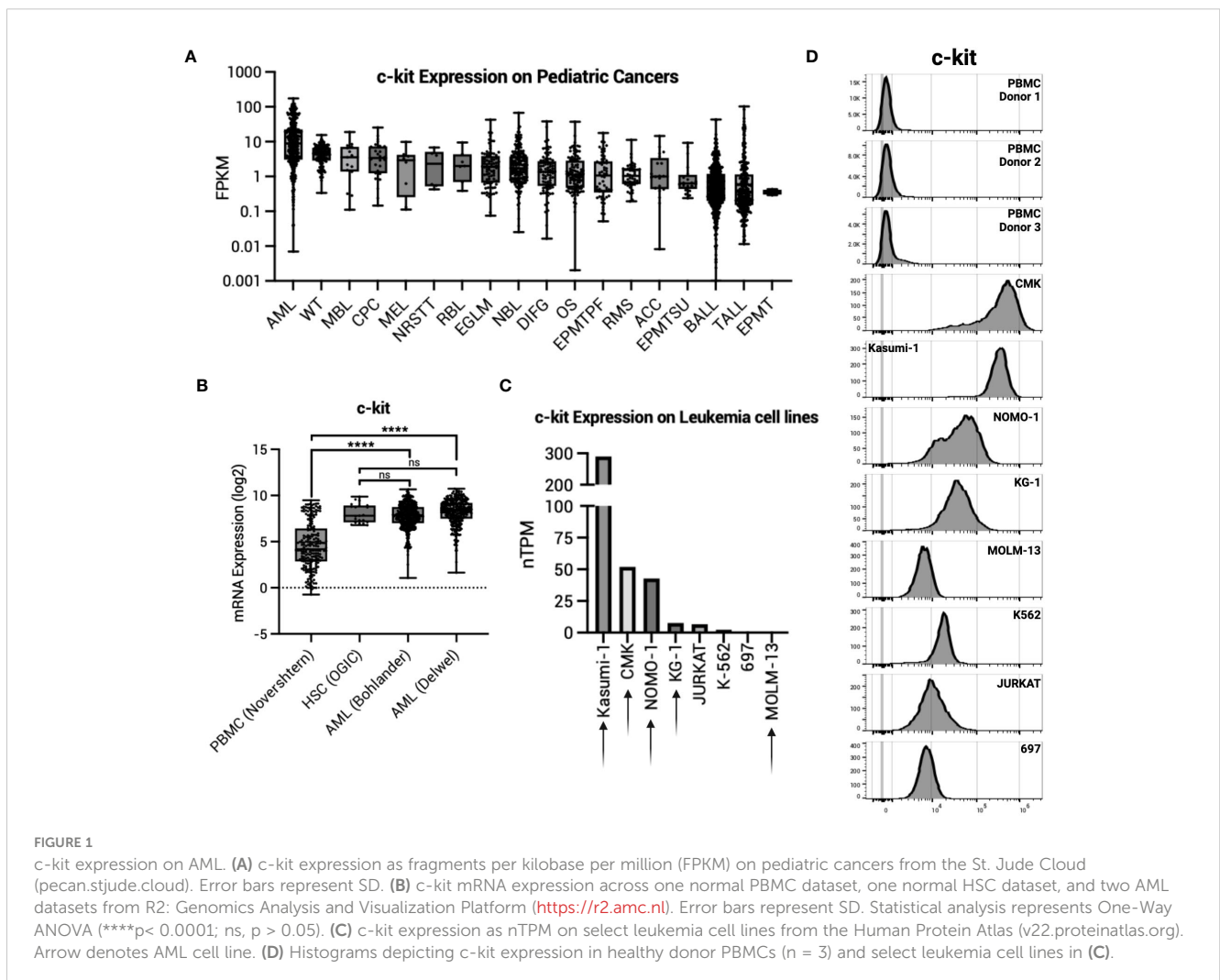
undetectable *c-kit* expression in most adult human organs by immunohistochemistry (IHC). Exceptions to this include high protein expression in the cerebellum, medium protein expression in the female reproductive organs (breast, fallopian tubes, and ovary), lung, skin, and testis, and low protein expression in the kidney, colon, and rectum. Data from the St. Jude Cloud (pecan.stjude.cloud) show many pediatric malignancies have high *c-kit* expression, with AML as the highest (Figure 1A). High expression of *c-kit* is corroborated in adult AML samples taken at time of diagnosis, with expression significantly higher than normal PBMCs yet comparable to HSCs (Figure 1B). To validate these findings, we confirmed *c-kit* expression on eight specific leukemia cell lines (proteintlas.org) (Figure 1C) and by flow cytometry (Figure 1D). Four of five AML cell lines tested (AML cell lines denoted by arrows in Figure 1C) demonstrate high *c-kit* expression compared to three healthy donor PBMCs (Figure 1D).

3.2 mSCF CAR $\alpha\beta$ T cells induce AML cell death *in vitro*

To this end, we generated a ligand-based *c-kit* directed CAR (mSCF CAR) by lentiviral gene delivery. The CAR construct

includes full-length murine SCF followed by a CD8 α hinge, CD28 co-stimulatory domain, and CD3 ζ signaling domain (Figure 2A). We chose to use the murine sequence for SCF as it binds both the human and murine *c-kit* receptor (47), making it possible to evaluate both cancer eradication and off-tumor toxicities in a murine model.

The first transgene tested included a bicistronic lentiviral vector encoding for dual expression of eGFP by a P2A ribosomal skipping sequence as a transduction marker (Figure 2A). Binding of the murine *c-kit* receptor to the mSCF CAR can be determined using a murine *c-kit* receptor conjugated to a constant fragment (Fc; *c-kit*-Fc) (Figure S1A). Jurkat T cells were used to evaluate CAR protein expression, ability to bind the human *c-kit* receptor, and AML specificity, with antigen-irrelevant CD19 CAR as a control. Jurkat T cells transduced with mSCF CAR at multiplicities of infection (MOIs) 0.5 and 2.5 resulted in 18% \pm 0.4% and 49% \pm 0.3% GFP⁺ cells respectively, while cells transduced with the control CD19 CAR resulted in 57% \pm 0.2% and 92% \pm 0.1% GFP⁺ cells, respectively (Figure 2B). Importantly, binding of the *c-kit*-Fc to mSCF CAR-modified Jurkat T cells results in CD69 upregulation and subsequent activation increasing with increasing MOIs, but not in CD19 CAR-modified Jurkat T cells (Figure 2C). Interestingly,



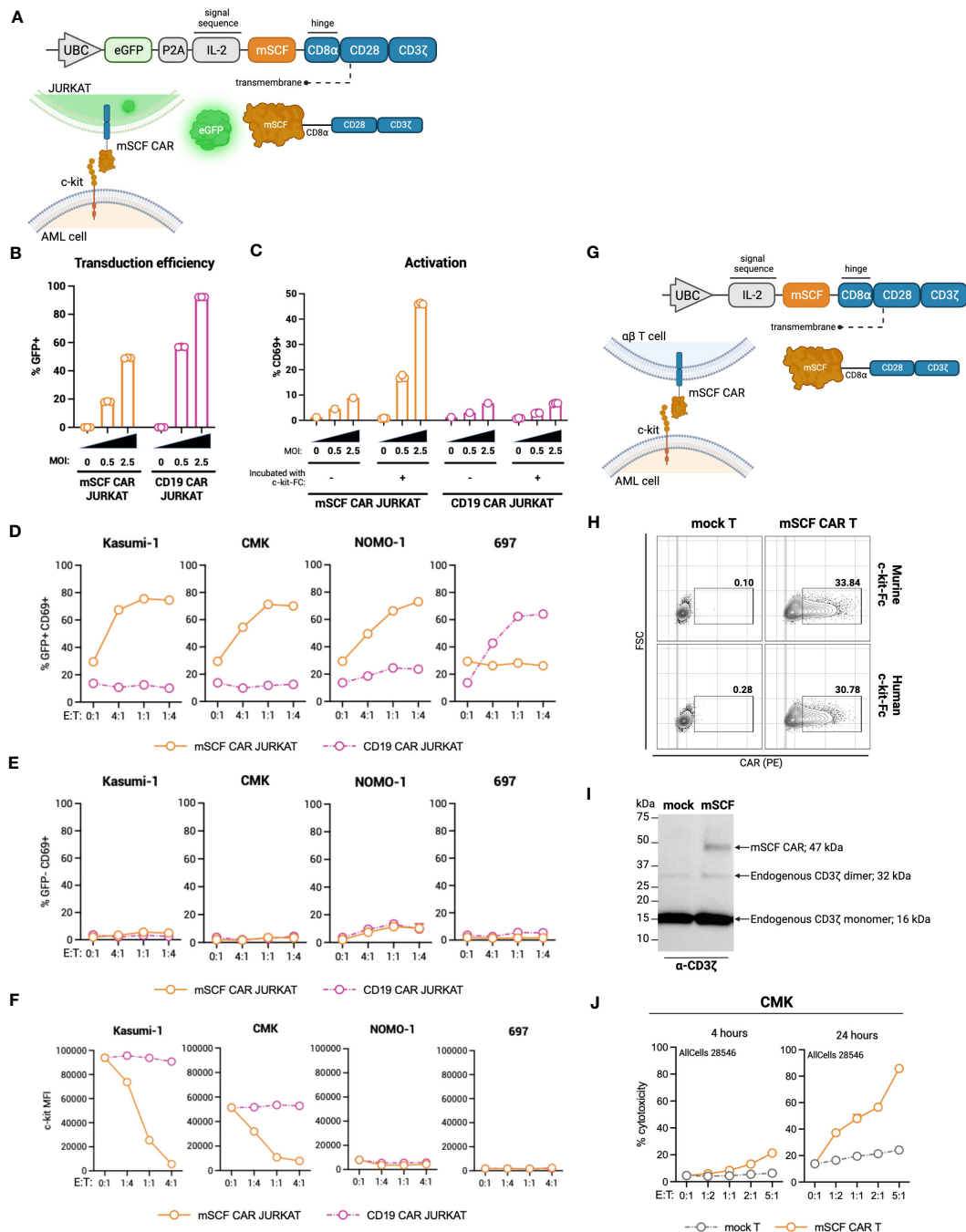


FIGURE 2

Design of novel ligand-based mSCF CAR and modification of $\alpha\beta$ T cells. (A) Schematic of lentiviral GFP mSCF CAR DNA construct. (B) Transduction efficiency as depicted by %GFP⁺ live Jurkat T cells. Error bars represent SD. n = 3 experimental replicates. (C) Activation of live mSCF CAR- or CD19 CAR-modified Jurkat T cells as depicted by %CD69⁺ when stained with 20 ng murine c-kit-Fc chimera. Error bars represent SD. n = 1-3 experimental replicates. (D) %CD69 activation of live mSCF CAR- or CD19 CAR-modified GFP⁺ Jurkat T cells when co-cultured with 4 different leukemia cell lines at 4 different effector-to-target (E:T) ratios. Error bars represent SD. n = 2 experimental replicates. (E) %CD69 activation of live un-modified GFP- Jurkat T cells under the same conditions as (D). Error bars represent SD. n = 2 experimental replicates. (F) c-kit MFI of 4 leukemia cell lines when co-cultured with mSCF CAR- or CD19 CAR-modified Jurkat T cells under the same conditions as (D). Error bars represent SD. n = 2 experimental replicates. (G) Schematic of lentiviral mSCF CAR DNA construct without GFP marker. (H) Representative flow plots depicting mSCF CAR expression on primary T cells transduced at MOI 20 when stained with 20 ng of murine or human c-kit-Fc chimera. (I) Western blot depicting CAR expression from whole cell lysates of primary T cells transduced with mSCF CAR at MOI 20. Western blot antibody against human CD3 ζ . (J) Four- and 24-hour flow cytometry cytotoxicity assays of mSCF CAR-modified primary T cells against c-kit expressing AML cell line CMK compared to mock T cell controls. Percent cytotoxicity is the sum of 7AAD⁺, Annexin V⁺, and 7AAD⁺ Annexin V⁺ cells when gated on VPD450-stained target cells only. Error bars represent SD. n = 2 experimental replicates with 1 donor.

this increase in activation is only seen when both c-kit-Fc and secondary F(ab')₂ are used (Figure S2B), suggesting multiple binding domains of the secondary F(ab')₂ may potentially induce CD3 ζ cross-linking among CAR molecules (Figure S1C), though further evidence is required.

To assess interaction of the mSCF CAR with human c-kit and the ability to activate Jurkat T cells, mSCF CAR Jurkat T cells were co-cultured with c-kit⁺ human cell lines Kasumi-1, CMK, and Nomo-1 at various effector-to-target (E:T) ratios, with the B-cell leukemia cell line 697 as an antigen-negative control, as it does not express c-kit. CD19 CAR Jurkat T cells were used as an antigen-irrelevant control for co-cultures with c-kit⁺ cell lines, as they do not express CD19, and a positive control when co-cultured with 697 cells, as 697 cells do express CD19. Indeed, transduced (GFP⁺) Jurkat T cells resulted in increased CD69⁺ activation when co-cultured with their antigen-matched target cells (Figure 2D), while un-transduced (GFP⁻) Jurkat T cells do not exhibit increased CD69⁺ activation (Figure 2E). Furthermore, it is known that interaction of SCF with the c-kit receptor causes receptor internalization (48). Indeed, co-culture of mSCF CAR Jurkat T cells with c-kit⁺ cell lines resulted in decreased c-kit MFI, while MFI remain unchanged when target cells were co-cultured with CD19 CAR Jurkat T cells (Figure 2F).

As a ligand-based therapeutic, it is important to consider the consequences of CAR shedding, as additional SCF in circulation may promote cancer cell proliferation (48). To assess CAR shedding, c-kit⁺ AML cell lines CMK and Kasumi-1 were incubated with media from mSCF CAR $\alpha\beta$ T cells or CD19 CAR $\alpha\beta$ T cells, with mock $\alpha\beta$ T cells as a control. As a positive control, cell lines were incubated with T cell media supplemented with recombinant murine SCF to induce receptor internalization. After a 15-minute incubation, there is no evidence of receptor internalization when cells were incubated with mSCF CAR media, suggesting the mSCF CAR is not shed from the surface of the cell at levels sufficient to influence surface c-kit levels (Figure S2).

To investigate the mSCF CAR in a more clinically relevant setting, we tested a second lentiviral mSCF CAR transgene cassette that had eGFP removed in primary $\alpha\beta$ T cells (Figure 2G). Primary $\alpha\beta$ T cells were transduced at MOI 20, after which binding of mSCF CAR $\alpha\beta$ T cells to both murine and human c-kit-Fc was confirmed by flow cytometry (Figure 2H) and overall protein expression was confirmed by western blotting against CD3 ζ (Figure 2I). To assess cytotoxicity, mSCF CAR $\alpha\beta$ T cells were co-cultured with c-kit⁺ CMK cells at increasing E:T ratios for 4- or 24-hours and showed increased cytotoxicity compared to mock $\alpha\beta$ T controls (Figure 2J). Specifically, after 24-hours of co-culture, mSCF CAR $\alpha\beta$ T cells induced cytotoxicity to an average of 37% at a 1:2, 48% at a 1:1, 57% at a 2:1, and 86% at a 5:1 E:T ratio. Together, these data show mSCF CAR T cells induce efficient and c-kit-specific killing of c-kit⁺ AML cell lines *in vitro*.

3.3 mSCF CAR $\alpha\beta$ T cells expand *in vivo* in the absence of AML

To identify possible toxicities of mSCF CAR $\alpha\beta$ T cells *in vivo*, NOD.Cg-Prkdc^{scid}Il2rg^{tw1Wjl}/SzJ (NSG) mice were administered

5×10^6 total mSCF CAR-modified $\alpha\beta$ T cells by tail-vein injection. To assess clonal expansion of the CAR⁺ population *in vivo*, $\alpha\beta$ T cells were transduced at low MOIs, providing approximately 8% CAR⁺ cells (Figure 3A). Six weeks after administration of T cells, mice were sacrificed to assess clonal expansion of CAR⁺ cells in the peripheral blood, spleen, and bone marrow compartments by flow cytometry. Significantly more CAR⁺ $\alpha\beta$ T cells were found in the bone marrow ($26\% \pm 6\%$) than in the peripheral blood ($5\% \pm 1\%$) (Figure 3B), with the percentage of CAR⁺ cells found in the peripheral blood closely resembling percent CAR⁺ cells injected at the beginning of the study.

To test clonal expansion in the presence of AML cells, NSG mice were first subjected to 100 rads of x-ray irradiation, then inoculated with 5×10^6 luciferase-modified CMK cells by tail-vein injection. The following day, mice were intravenously injected with one dose of 5×10^6 total mock or mSCF CAR $\alpha\beta$ T cells (8% CAR⁺). Three weeks later, circulating human CD3⁺ T cells were significantly higher in mSCF CAR $\alpha\beta$ T-cell treated mice ($48\% \pm 26\%$) compared to mock $\alpha\beta$ T-cell treated mice ($18\% \pm 18\%$) (Figure 3C). No expansion of CAR⁺ cells was observed in the periphery, as only $7\% \pm 3\%$ CAR⁺ cells were found in circulation three-weeks after injection, resembling the percentage of CAR⁺ cells in the injected product (Figure 3D).

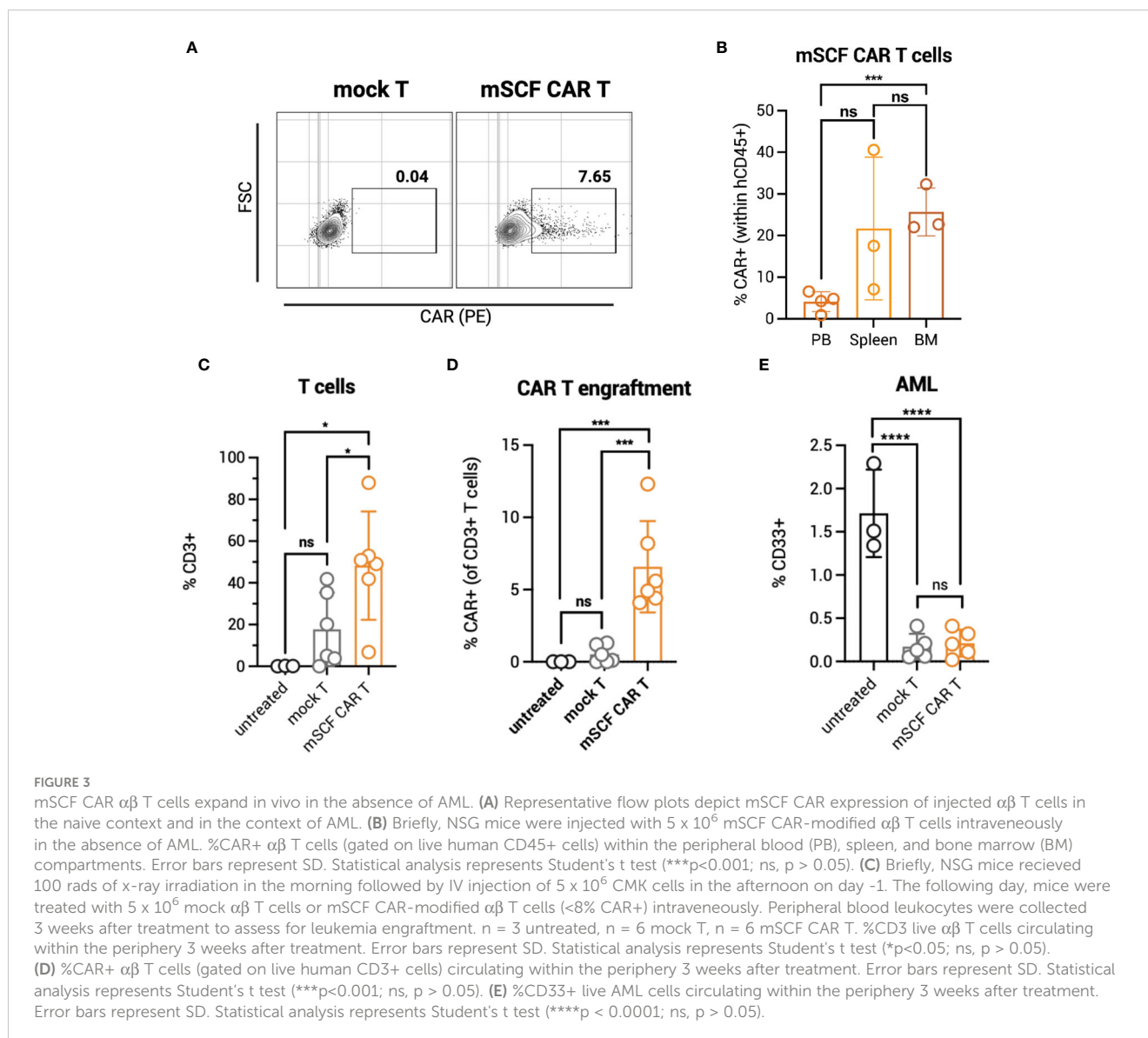
CD33⁺ AML burden in the periphery was significantly decreased in mSCF CAR-treated mice ($0.2\% \pm 0.2\%$) compared to untreated controls ($2\% \pm 0.5\%$) three-weeks after treatment, though not significantly different than mock $\alpha\beta$ T-cell treated mice ($0.2\% \pm 0.2\%$) (Figure 3E). However, despite a lack of difference in AML burden in the periphery between treatment groups, mSCF CAR $\alpha\beta$ T cell treated mice met endpoint criteria significantly sooner than untreated or mock $\alpha\beta$ T treated mice, suggesting greater toxicity *in vivo* despite low CAR transduction (Figure S3).

Though we did not observe clonal expansion of CAR⁺ $\alpha\beta$ T cells in the periphery of AML bearing mice, we hypothesized there could be clonal expansion in other hematopoietic organs with high c-kit expression, such as the bone marrow. Despite promising *in vitro* data, we determined that mSCF CAR-modified $\alpha\beta$ T cells induced excessive toxicity *in vivo* even at low modification efficiency. Thus, we sought additional safety modifications in our design.

3.4 c-kit-targeting $\gamma\delta$ T cells induce AML cell death *in vitro*

$\gamma\delta$ T cells have an innate ability to recognize stress antigens through NKG2D expression (49). NKG2D ligands—MICA/MICB and ULBP1-6—interact with NKG2D on $\gamma\delta$ T cells and activate innate killing mechanisms (50). Primary AML samples taken at time of diagnosis from two different datasets express significantly higher transcript levels of NKG2D ligands MICA/MICB, ULBP1, and ULBP2 compared to healthy PBMC control (Figures 4A–C). These results were corroborated with cell surface expression on AML cell lines as measured by flow cytometry (Figures 4D–F).

To test c-kit-directed ligand-based therapeutics in $\gamma\delta$ T cells, we developed a transgene to express the mSCF CAR under a T7 promoter for mRNA production (Figure 5A). Similarly, we also



developed a ligand-based secreted bispecific T-cell engager (sBite) using the human sequence for SCF and an anti-CD3 scFv (clone: OKT3) (Figure 5B). When expressed in a $\gamma\delta$ T cell, the hSCF sBite is secreted and dually binds to the $\gamma\delta$ T-cell receptor (TCR) and c-kit, which is expressed on the target cell, and induces cytotoxicity. As $\gamma\delta$ T cells have innate cytotoxicity against cancer cells, we posited that expressing these targeted transgenes transiently would provide potent tumor clearance without long-term off-target toxicities within the c-kit compartment. Flow cytometric analysis confirms CAR surface expression using mouse and human c-kit-Fc (Figure 5C). Interestingly, $\gamma\delta$ T cells modified with the hSCF sBite shift positively when incubated with the human c-kit-Fc, suggesting sBite secretion, binding to surface CD3e and ability to bind to human c-kit. Importantly, this also confirms that the human sequence for SCF is unable to bind to murine c-kit (Figure 5C). Overall, mSCF CAR transfection efficiency averages to $63\% \pm 18\%$ from samples across eight healthy donors (Figure 5D).

To assess cytotoxicity of mSCF CAR and hSCF sBite-modified $\gamma\delta$ T cells, human AML cell lines CMK and Kasumi-1 were co-cultured for 4-hours with mock $\gamma\delta$ T cells, mSCF CAR $\gamma\delta$ T cells, or hSCF sBite $\gamma\delta$ T cells at increasing E:T ratios (Figure 5E). As expected, the degree of toxicity of non-modified $\gamma\delta$ T cells against some AML cell lines is donor dependent (35). Cytotoxicity increased as E:T ratios increased across the three donors to variable degrees and importantly, CAR and sBite modification enhanced cytotoxicity in all donors (Figure 5E). To further confirm secretion of the hSCF sBite from modified $\gamma\delta$ T cells, c-kit⁺ CMK cells were co-cultured with mock $\gamma\delta$ T cells, mock $\gamma\delta$ T cells supplemented with hSCF sBite conditioned media, or hSCF sBite-modified $\gamma\delta$ T cells at increasing E:T ratios. Mock $\gamma\delta$ T cells supplemented with hSCF sBite conditioned media induced the same degree of cytotoxicity as hSCF sBite-modified $\gamma\delta$ T cells, indicating the hSCF sBite is secreted into the media and can act on both modified and non-modified cells (Figure 5F).

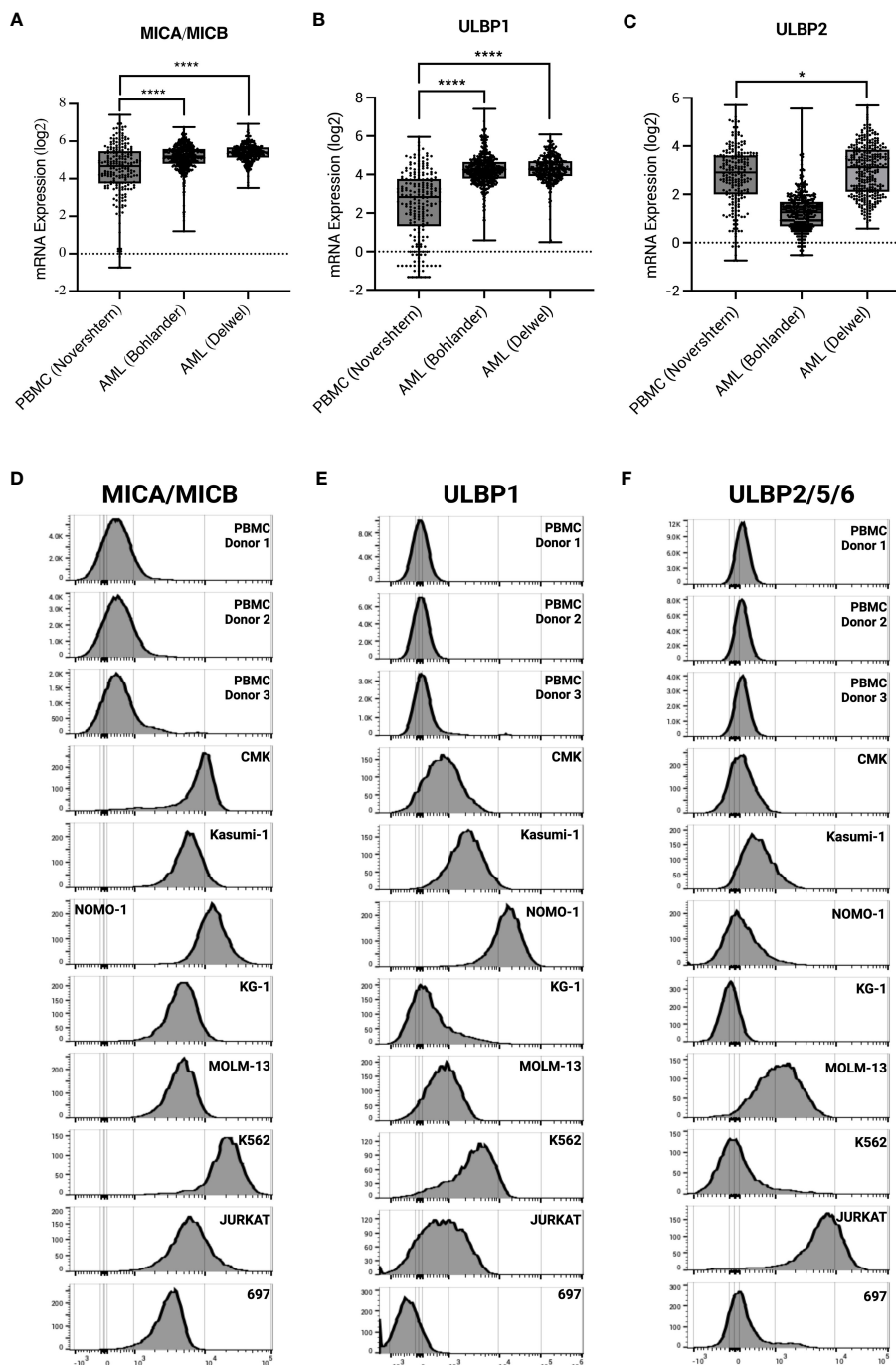


FIGURE 4
 AML and leukemia cell lines express stress antigens MICA/MICB, ULBP1, and ULBP2/5/6. mRNA expression of stress antigens MICA/MICB (A), ULBP1 (B), and ULBP2 (C) on normal PBMC and two AML datasets queried using R2: Genomics Analysis and Visualization Platform (<https://r2.amc.nl>). Error bars represent SD. Statistical analysis represents One-Way ANOVA (**** $p < 0.0001$; * $p < 0.05$). Histograms depict stress antigen expression of MICA/MICB (D), ULBP1 (E), and ULBP2/5/6 (F) in healthy donor PBMC ($n = 3$) and leukemia cell lines by flow cytometry.

3.5 c-kit-targeting mSCF CAR $\gamma\delta$ T cells induce sca-1⁺ cell death ex vivo

While hSCF sBite-modified $\gamma\delta$ T cells should not induce toxicity against murine c-kit⁺ cells in the bone marrow, as human SCF does not bind to murine c-kit, it is still important

to consider the toxicity of mSCF CAR-modified $\gamma\delta$ T cells against murine c-kit⁺ cells in the bone marrow. To accomplish this, mSCF CAR $\gamma\delta$ T cells and hSCF sBite $\gamma\delta$ T cells were co-cultured for 24-hours with sca-1⁺ isolated murine bone marrow at an E:T ratio of 1:2. Importantly, cells were co-cultured in both the absence and presence of supraphysiological levels of recombinant murine SCF

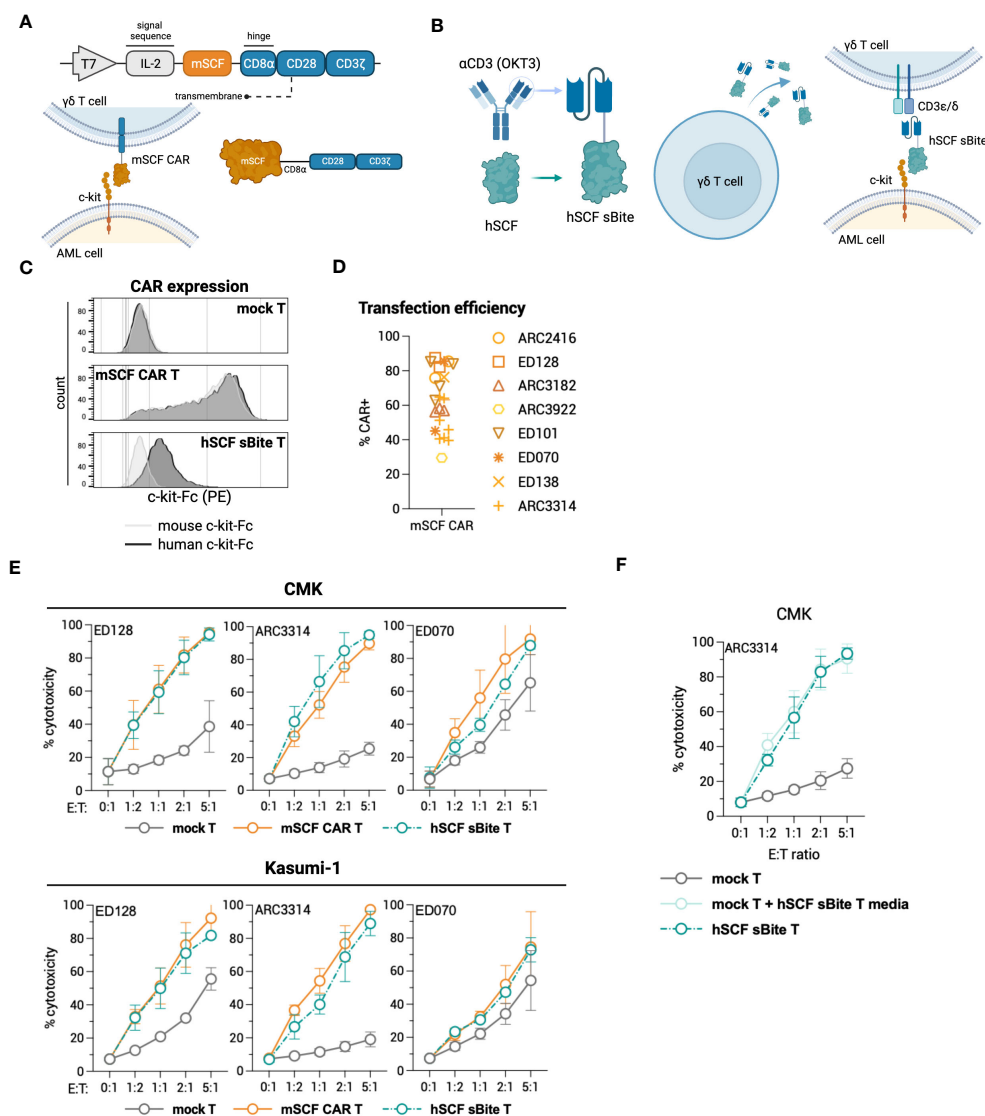


FIGURE 5
 Design of novel ligand-based therapeutics and transient modification of $\gamma\delta$ T cells. **(A)** Schematic of mSCF CAR construct for mRNA generation. **(B)** Diagram of hSCF sBite construct for mRNA generation. **(C)** Representative flow plots depicting mSCF CAR expression on primary $\gamma\delta$ T cells transfected with 15 μ g mRNA encoding denoted construct when stained with 20 ng of murine or human c-kit-Fc chimera. **(D)** Pooled transfection efficiency of primary $\gamma\delta$ T cells modified with the mSCF CAR. n = 8 donors with n = 1-7 biological replicates. **(E)** Four-hour flow cytometry cytotoxicity assays of mSCF CAR- and hSCF sBite-modified primary $\gamma\delta$ T cells against c-kit expressing AML cell lines compared to mock $\gamma\delta$ T cell controls. Percent cytotoxicity is the sum of 7AAD⁺, Annexin V⁺, and 7AAD⁺ Annexin V⁺ cells when gated on VPD450-stained target cells only. Error bars represent SD. n = 3 donors with n = 2-7 biological replicates each. **(F)** Four-hour flow cytometry cytotoxicity assay of hSCF sBite $\gamma\delta$ T cells against c-kit⁺ CMK cells compared to mock $\gamma\delta$ T cell control. Mock $\gamma\delta$ T cells were co-cultured with media from hSCF sBite-modified cells and c-kit⁺ CMK cells to measure sBite secretion. Error bars represent SD. n = 1 donor with n = 4 biological replicates.

to assess the functionality of a ligand-based therapy in a ligand competing environment.

After 24-hours, mSCF CAR $\gamma\delta$ T cells, but not hSCF sBite or mock $\gamma\delta$ T cells, reduced the c-kit⁺ and Lineage⁻ sca-1⁺ c-kit⁺ (LSK) compartments of murine bone marrow (Figures 6A, B). A colony forming unit (CFU) assay cultured at a 1:2 E:T ratio confirms a depletion of progenitor cells in only the cells co-cultured with mSCF CAR $\gamma\delta$ T cells (Figure 6C). Importantly, this depletion can be seen in both the presence and absence of recombinant murine SCF, suggesting ligand competition inhibiting functionality is minimal.

3.6 $\gamma\delta$ T cells have limited persistence in NSG mice

Given enhanced toxicity of mSCF CAR $\gamma\delta$ T cells *ex vivo*, and the *in vivo* expansion of $\alpha\beta$ T cells in murine bone marrow, we next determined $\gamma\delta$ T-cell kinetics *in vivo* to evaluate possible bone marrow toxicity. To this end, NSG mice were injected with 10⁷ $\gamma\delta$ T cells by intravenous, retro-orbital injection and peripheral blood leukocytes were collected once daily for 4 days (Figure 7A). To determine if IL-2 or zoledronic acid enhanced *in vivo* persistence, a treatment regimen of two doses of 13,000 IU recombinant human

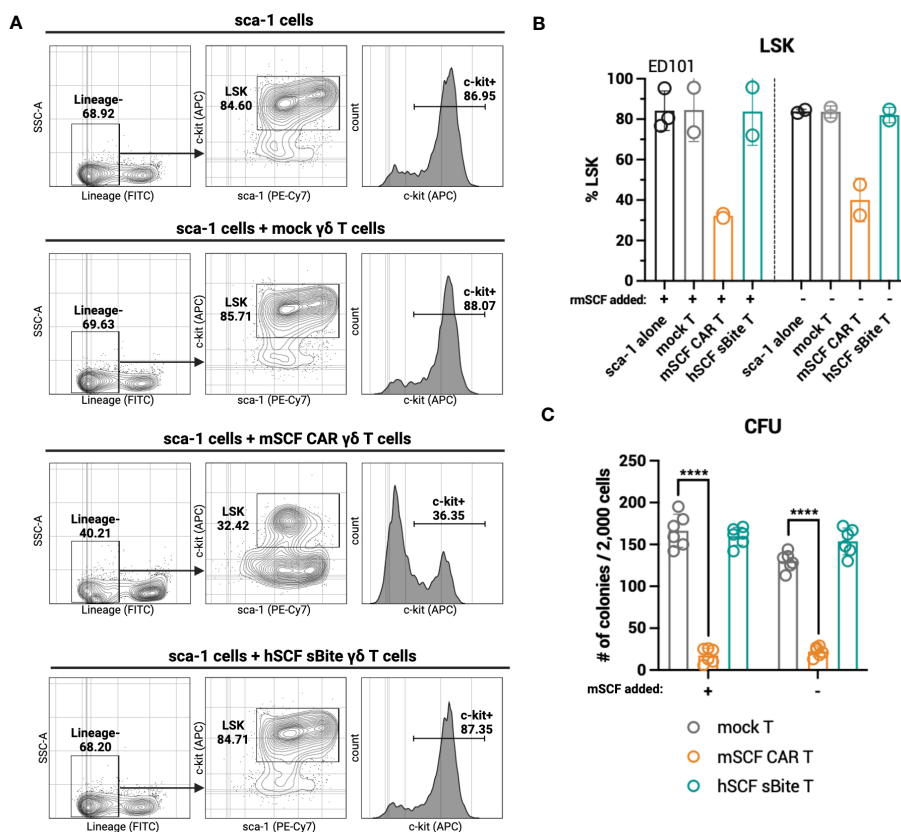


FIGURE 6 mSCF CAR-modified $\gamma\delta$ T cells, but not hSCF sBite-modified $\gamma\delta$ T cells, are cytotoxic against murine bone marrow *ex vivo*. (A–C) Briefly, murine sca-1⁺ cells were harvested from bone marrow of C57BL/6 mice, rested for 1 day in media supplemented with mIL-3 (20 ng/mL), hIL-11 (100 ng/mL), and hFlt3 (100 ng/mL) and with or without mSCF (100 ng/mL), then co-cultured with $\gamma\delta$ T cells for 24-hours at a 1:2 E:T ratio. Co-cultures were subject to flow cytometry analysis to assess LSK and c-kit⁺ compartments. (A) Representative flow plots depict LSK and c-kit⁺ compartments of murine sca-1⁺ cells in a 24-hour *ex vivo* co-culture of mock $\gamma\delta$ T cells, mSCF CAR $\gamma\delta$ T cells, or hSCF sBite $\gamma\delta$ T cells supplemented with all cytokine excluding mSCF. (B) %LSK (gated on live hCD3⁺ h $\gamma\delta$ TCR⁻ cells). Error bars represent SD. n = 2–3 biological replicates. (C) Number of colonies counted from colony forming unit (CFU) assay after 24-hour co-culture. Error bars represent SD. n = 3 technical replicates. n = 2 biological replicates.

IL-2 by intraperitoneal injection and one dose of 70 μ g/kg zoledronic acid by subcutaneous injection or two doses of IL-2 alone were given. Percent $\gamma\delta$ T cells were highest in circulation 48 hours after injection, with a steady decline in persistence up to 4 days after injection (Figure 7B). $\gamma\delta$ T cells were found in the spleen (Figure 7C) and bone marrow 4 days after injection, though very low levels were found in the bone marrow (Figure 7D). Neither treatment with IL-2 or combination IL-2 and zoledronic acid treatment enhanced $\gamma\delta$ T-cell persistence.

The lack of $\gamma\delta$ T cells infiltrating the extravascular bone marrow space of NSG mice may prove advantageous to control on-target off-tumor toxicity in the bone marrow compartment. To investigate this further, we directly injected mSCF CAR $\gamma\delta$ T cells into the left femur of NSG mice, with mock $\gamma\delta$ T cells as a control, and assessed for bone marrow clearance two days later, when $\gamma\delta$ T cells have previously been shown to be at their highest in circulation. Indeed, human CD3⁺ human $\gamma\delta$ TCR⁺ $\gamma\delta$ T cells were found in the peripheral blood and spleen two days after injection (Figures 7E–G). However, only a small number $\gamma\delta$ T cells remained in the injected left femur (Figure 7G). Additionally, changes in the c-kit⁺ compartment of the peripheral blood, spleen, and bone marrow of

the left and right femur were not observed between groups (Figures 7H–J). A CFU assay confirmed no changes in progenitor cell populations between the left (injected) and right (control) femur (Figure 7K).

Together, these data show $\gamma\delta$ T cells do not persist beyond four days in NSG mice and do not efficiently infiltrate the extravascular bone marrow compartment. This, in addition to transient transgene expression, can serve as a safety mechanism to limit toxicity.

3.7 hSCF sBite-modified $\gamma\delta$ T cells moderately improve survival *in vivo*

To assess efficacy against AML *in vivo*, NSG mice were first pre-conditioned with busulfan, then 5×10^6 luciferase-expressing CMK cells were established by intravenous injection the following morning. Beginning that afternoon, and for the next 3 days for a total of 4 doses, 1×10^7 total mSCF CAR $\gamma\delta$ T cells or hSCF sBite $\gamma\delta$ T cells were injected intravenously, with mock $\gamma\delta$ T cells as a control (Figure 8A). Bioluminescence was assessed regularly throughout the study (Figure 8B).

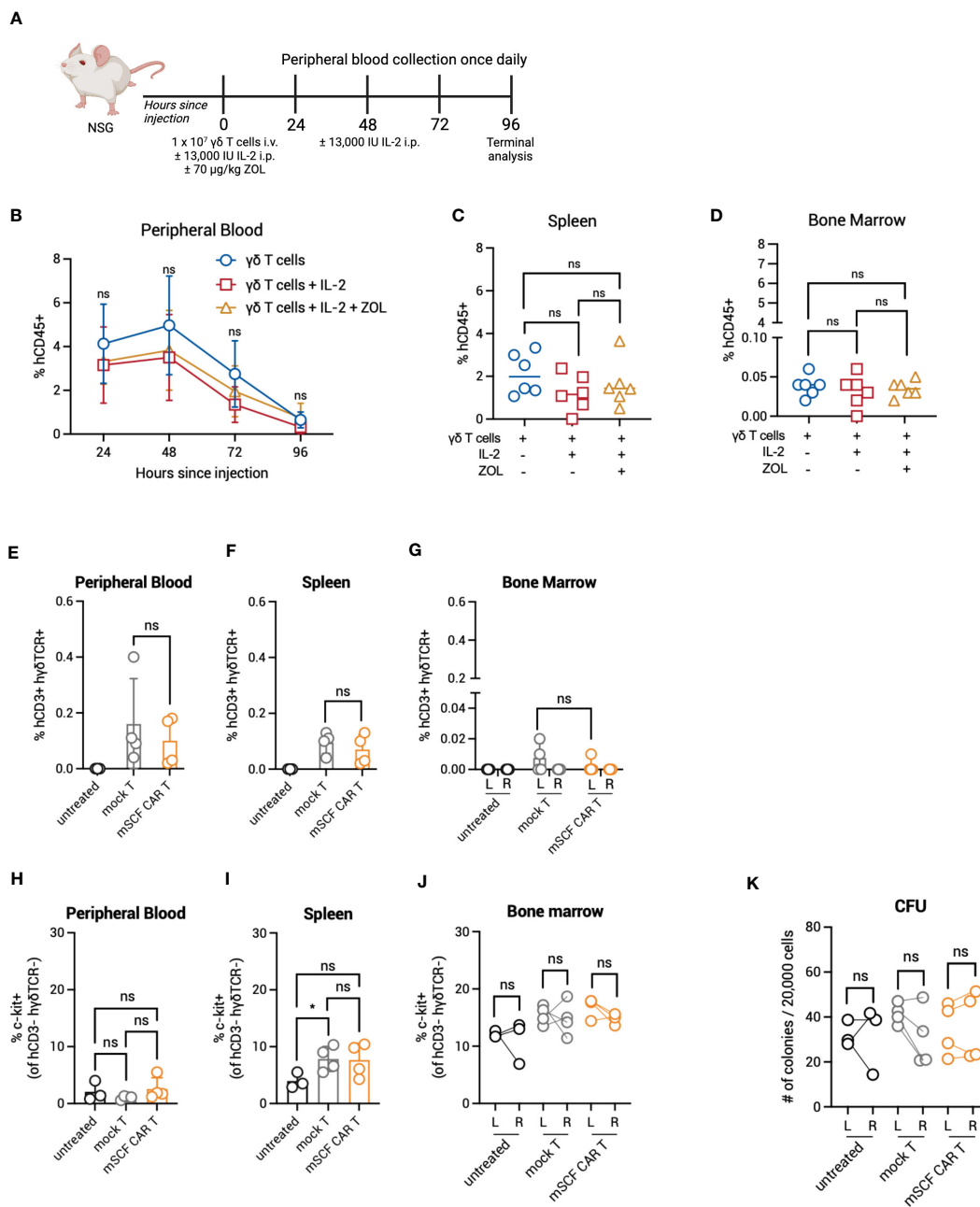


FIGURE 7

Persistence and toxicity of mSCF CAR $\gamma\delta$ T cells in immunocompromised mice. (A) Schematic. NSG mice were injected with 1×10^7 $\gamma\delta$ T cells IV alone on day 0 ($n = 6$), 1×10^7 $\gamma\delta$ T cells IV on day 0 and two doses of 13,000 IU IL-2 IP on day 0 and day 2 ($n = 6$), or 1×10^7 $\gamma\delta$ T cells IV on day 0, two doses of 13,000 IU IL-2 IP on day 0 and day 2, and one dose of 70 $\mu\text{g}/\text{mg}$ zoledronic acid SC on day 0 ($n = 6$). Peripheral blood leukocytes were collected daily beginning 24-hours after the start of treatment and assessed for the presence of human $\gamma\delta$ T cells. Four days later, mice were sacrificed to assess for human $\gamma\delta$ T cells within the spleen and bone marrow. (B) %hCD45+ (gated on live cells) within the peripheral blood at each timepoint. Error bars represent SD. Statistical analysis represents Student's t test (ns, $p > 0.05$). (C–D) %hCD45+ (gated on live cells) within the spleen (C) and bone marrow (D) at end point. Statistical analysis represents Student's t test (ns, $p > 0.05$). (E–G) %hCD3+ h $\gamma\delta$ TCR+ (gated on live cells) within the peripheral blood (E), spleen (F), and the left and right femurs (G). Error bars represent SD. Statistical analysis represents Student's t test (ns, $p > 0.05$). (H–J) %c-kit+ (gated on hCD3- h $\gamma\delta$ TCR- live cells) within the peripheral blood (H), spleen (I), and left and right femurs (J). Error bars represent SD. Statistical analysis represents unpaired (H, I) or paired (J) Student's t test (* $p < 0.05$; ns, $p > 0.05$). (K) Number of colonies counted from a CFU assay on the left and right femurs. Statistical analysis represents paired Student's t test (ns, $p > 0.05$). Data point graphed is averaged from $n = 3$ technical replicates per mouse.

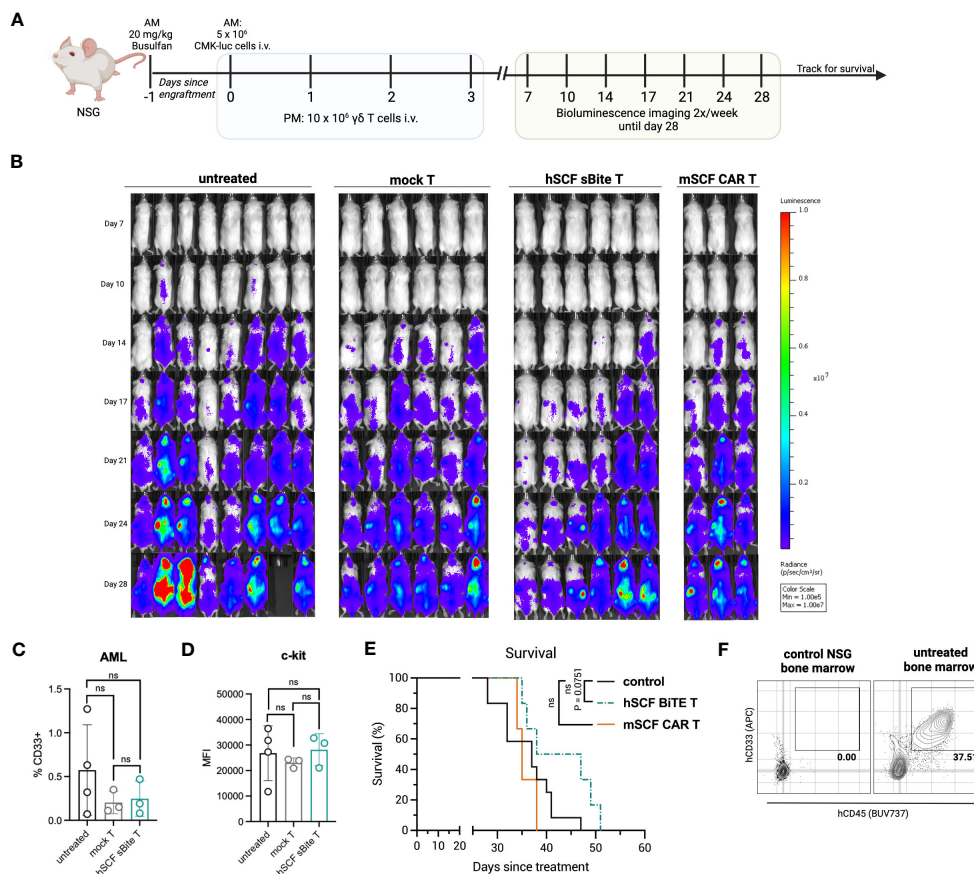


FIGURE 8

Treatment of hSCF sBite-modified $\gamma\delta$ T cells only moderately prolongs survival *in vivo*, despite aggressive treatment regimen. (A) Experimental design. Briefly, NSG mice were pre-conditioned with 20 mg/kg busulfan IP on day -1, then injected with 5×10^6 CMK cells via tail-vein injection in the morning on day 0. Beginning in the afternoon on day 0, and then once daily for the next 3 days for a total of 4 doses, 1×10^7 $\gamma\delta$ T cells were injected via tail-vein injection. Mice were subjected to bioluminescence imaging for the following 3 weeks, then followed for survival until they met endpoint. $n = 8$ untreated, $n = 6$ mock T treated, $n = 6$ hSCF sBite treated, $n = 3$ mSCF CAR treated. (B) Bioluminescence images. (C) Peripheral blood leukocytes were collected 3 weeks after the start of treatment and assessed for presence of CD33⁺ CMK cells. Error bars represent SD. Statistical analysis represents Student's t test (ns, $p > 0.05$). (D) MFI of c-kit on CMK cells within the periphery. Statistical analysis represents Student's t test (ns, $p > 0.05$). (E) Kaplan-Meier survival analysis. Untreated and mock $\gamma\delta$ T treated groups were combined as a control group. Statistical analysis represents log rank (Mantel-Cox) test (ns > 0.05). P-value is shown. (F) Representative flow plots of hCD33⁺ hCD45⁺ CMK cells in the bone marrow of an untreated mouse sacrificed near end-point.

There was a clear delay in cancer development in hSCF sBite $\gamma\delta$ T cell-treated mice that was not observed in mSCF CAR $\gamma\delta$ T cell-treated mice (Figure 8B). We postulate this suppression of growth despite similar *in vitro* results can be attributed to the secretion of the hSCF sBite and its ability to engage all $\gamma\delta$ T cells, whereas the mSCF CAR can only function through transfected cells as it is a surface-bound protein.

Three weeks after the establishment of AML, peripheral blood leukocytes were collected and subject to flow cytometry analysis for the presence of CD33⁺ CMK cells. At this time, there were few CMK cells in the peripheral blood, especially in mSCF CAR and hSCF sBite treated mice (Figure 8C). The mean percentage of CMK cells was lower in CAR and sBite treated mice compared to untreated mice (0.3% vs 0.6%), however the differences did not approach significance (Figure 8C). The surface expression of c-kit, as measured by MFI, on circulating CMK cells did not differ among groups, suggesting antigen escape is not a mechanism of immune evasion (Figure 8D). Complete blood counts (CBCs) did not show significant differences among groups, though all

mice experienced thrombocytopenia, which was likely due to cancer progression affecting hematopoiesis (Figures S4A–H).

Treatment with mSCF CAR did not result in a significant survival benefit under the conditions tested, whereas hSCF sBite $\gamma\delta$ T cells showed a trend towards survival enhancement (Figure 8E, $p = 0.075$). One possibility as a mechanistic explanation for the discrepancy between the efficient *in vitro* cytotoxicity and *in vivo* tumor clearance is the observation that surviving CMK cells were primarily observed in the extravascular bone marrow compartment (Figure 8F). We have previously shown that $\gamma\delta$ T cells do not readily migrate to murine bone marrow (39), possibly due to minimal CXCR4 expression (Figure S5), an important chemokine receptor that helps leukocytes migrate from the periphery to the bone marrow (51). Taken together, these data suggest CMK cell growth is inhibited at early time points when injected into peripheral circulation up until they leave circulation and populate the bone marrow, where even high doses of $\gamma\delta$ T cells cannot control disease burden in the extravascular bone marrow compartment.

4 Discussion

AML proves more difficult to manage with targeted therapeutics, such as CAR T therapy, than B-cell malignancies due to a scarcity of cancer-specific target receptors. Despite this, preclinical efforts to develop CAR T therapies for AML are ongoing and include targets such as CD33 (14), CD123 (52, 53), and CD70 (54). Most notably, therapeutics targeting CD33 (NCT03971799) and CD123 (NCT04678336) have advanced to clinical trials and show some clinical promise. However, critical measures are needed to mitigate off-target toxicities of these therapies within the bone marrow niche, as HSCs express both CD33 and CD123. As HSCT is curative for patients with AML and toxicities associated with pre-transplantation conditioning are severe (8), it has been observed that these toxicities may be advantageous and can even replace pre-transplantation conditioning.

C-kit, or CD117, has also been explored as a potential target for the development of CAR T therapy in the context of AML (22, 55). As c-kit is expressed on HSCs, current therapeutics targeting c-kit have been designed as a bridge-to-transplant by eradicating HSCs and leukemia simultaneously. Indeed, preclinical studies targeting c-kit as a means of pre-transplantation conditioning alone using antibody-immunotoxin conjugates by our lab (17) and others (18) and using CAR T cells (21) are ongoing. Clinically, briquilimab has shown promise in a Phase 1/2 dose-escalation trial of patients undergoing HSCT for severe combined immunodeficiency (SCID; NCT02963064) and a Phase 1 trial of patients undergoing HSCT for MDS/AML (NCT04429191).

Herein, we designed a ligand-based CAR and sBite to target c-kit using its cognate ligand SCF for the treatment of AML. The reasons for choosing a ligand-based design over a traditional scFv are many. Primarily, the elimination of stabilizing interactions that exist in the original antibody structure and simultaneous introduction of a non-native linker sequence between the variable heavy and light domains can result in thermal instability, partial scFv unfolding, domain swapping, and uncontrolled heterodimerization between two scFv molecules (27, 56). Therefore, to ensure stability of the antigen-binding domain and prevent scFv aggregation leading to tonic signaling of the CAR or inefficiency of the sBite, we tested a ligand-based design. It is true that some ligands, such as SCF, have dimerization potential; however, this does not interfere with receptor binding (and, in turn, therapeutic efficacy), as ligand dimers may still bind their receptors, though it may lead to enhanced tonic signaling. In fact, this design may prove advantageous over a traditional scFv-based design due to differences in affinity of the binding domain to the receptor. While the binding affinity for human SCF to human c-kit is strong and falls within the nanomolar range (57), it is still weaker than that of an antibody-antigen interaction, which can fall as low as picomolar range (58). Recent studies suggest that low-affinity CAR T cells have a lower risk of antigen escape through decreased trogocytosis (59), increased tumor selectivity (60), reduced exhaustion (61), and a reduced risk of cytokine release syndrome (CRS) due to decreased cytokine secretion (61). Together, these benefits may promote an enhanced safety profile of the therapeutic and allow for the potential combination with other therapeutics.

That said, ligand-based therapeutics have been tested preclinically (62), with some advancing to clinical testing. For example, ligand-based IL-13R α 2-targeting CAR T cells whose binding domain utilizes a modified IL-13 ligand have shown promise for the treatment of childhood glioblastoma multiforme (GBM), resulting in tumor regression with enhanced IFN- γ signaling to activate the host immune system (63, 64).

The strategy of expressing CAR or sBite transgenes transiently in $\gamma\delta$ T cells (rather than traditional $\alpha\beta$ T cells) can serve as a safety modification and as a potential off-the-shelf therapeutic. $\gamma\delta$ T cells do not cause graft-versus-host-disease (GvHD) reactions when transplanted across HLA barriers, as $\gamma\delta$ T cells recognize antigen independent of HLA, while also contributing to graft-versus-leukemia (GvL) effect partially through the recognition of stress antigens (29–31). Importantly, pediatric patients with higher numbers of $\gamma\delta$ T cells after HSCT have significantly higher event-free survival, a lower probability of infection, and a lower risk of relapse, with the survival advantage lasting as long as 7 years after HSCT (65, 66). Additionally, $\gamma\delta$ T-cell infiltration into tumors has been identified as the most favorable prognostic factor in a pan-cancer analysis (67), further solidifying their clinical benefit.

We have been able to expand $\gamma\delta$ T cells *ex vivo* from healthy donors using a serum-free Good Manufacturing Practice (GMP) compliant expansion protocol (33, 35) and have shown preclinical efficacy in B-cell leukemia (39) and neuroblastoma models (32, 38). In fact, this manufacturing strategy is under clinical investigation in a Phase 1 trial in the context of childhood neuroblastoma (NCT05400603). With respect to AML, it is known that difficulties in manufacturing multiple doses and a lack of persistence of mRNA-based $\alpha\beta$ CAR T cells led to limited outcomes in clinical trials for anti-CD123 mRNA $\alpha\beta$ CAR T cells in patients with r/r AML (NCT02623582) (68). Concerns about manufacturing can be reduced by instead employing $\gamma\delta$ T cells as opposed to $\alpha\beta$ T cells, which can be manufactured from healthy donors and serve as an off-the-shelf therapeutic. Furthermore, transient expression of a c-kit-directed therapeutic may limit off-target toxicity in the bone marrow niche, and un-modified $\gamma\delta$ T cells can provide additional cancer surveillance through interaction with stress antigens, which we have shown are up regulated on AML cells.

In this study, c-kit-directed, ligand-based, mSCF CAR and hSCF sBite $\gamma\delta$ T cells were generated by mRNA electroporation, achieving >60% CAR modification on average. *In vitro*, we show mSCF CAR- and hSCF sBite-modified $\gamma\delta$ T cells are cytotoxic against c-kit⁺ AML cell lines, ablating >90% of AML cell lines during a short-term cytotoxicity assay at a low effector-to-target ratio. Furthermore, a significant decrease in the LSK compartment of murine bone marrow during a 24-hour *ex vivo* co-culture was shown with mSCF CAR-modified $\gamma\delta$ T cells, confirming the possibility of toxicity within the bone marrow compartment. Interestingly, this decrease in the LSK compartment was observed in both the absence and presence of supraphysiological levels of murine SCF and was confirmed by CFU assay, suggesting mSCF CAR $\gamma\delta$ T cells affected LSK pluripotency. One possible explanation for this surprising result is that while the addition of SCF to the co-culture may have initially protected LSK cells from $\gamma\delta$ T-cell

induced cell death by c-kit receptor internalization, subsequent re-expression of c-kit on the cell surface 12-14 hours later (69) may render them susceptible again, though more experiments are needed to test this hypothesis.

However, despite this toxicity *ex vivo*, it was not observed *in vivo*, likely due to limited trafficking of $\gamma\delta$ T cells to the bone marrow niche. As such, treatment of AML-bearing mice with hSCF sBite-modified $\gamma\delta$ T cells only slightly prolonged survival. This, in combination with previously published (38, 39, 70) and ongoing studies within our group, now defines an important limitation of studying human IL-2/zoledronic acid-expanded $\gamma\delta$ T cells in the murine setting, as these cells do not migrate to the bone marrow, which is the site of later stage CMK cell growth in this AML mouse model. Alternatively, it is also possible that the inefficient migration of human $\gamma\delta$ T cells into the murine extravascular bone marrow compartment may simply be due to specific-specific chemokine-receptor incompatibility. Despite this limitation, our data suggest that the hSCF sBite provides better control of tumor growth than the mSCF CAR, which can be attributed to the activation of both modified and non-modified cells, as the sBite is secreted and can interact with all CD3⁺ cells.

As many myeloid malignancies include bone marrow involvement, a lack of trafficking of $\gamma\delta$ T cells to the bone marrow niche proves challenging for clinical translation. Indeed, others have shown difficulty in trafficking of leukocytes to the bone marrow and have proposed the overexpression of CXCR4 by retroviral transduction as a means of enhancing trafficking (21). Another strategy may instead aim to enhance CXCR4 expression through modification of our expansion protocol, as it has been shown that the addition of TGF- β to expansion media upregulates CXCR4 on $\gamma\delta$ T cells (70, 71). However, to date, we have not been successful in repeating this finding, possibly due to our unique serum-free method of expansion. Further studies aim to enhance $\gamma\delta$ T-cell persistence in the bone marrow by similar modifications, and are currently underway. Despite these limitations, these data demonstrate ligand-based $\gamma\delta$ T-cell therapies targeting c-kit for the treatment of AML is fundamentally possible. Future investigation will focus on efforts to enhance $\gamma\delta$ T cell migration and infiltration into the bone marrow, and specifically address toxicities associated with hSCF sBite expression within the bone marrow compartment.

Data availability statement

The raw data supporting the conclusions of this article will be made available by the authors, without undue reservation.

Ethics statement

The studies involving humans were approved by the Institutional Review Board (IRB), Emory University, Atlanta, GA. The studies were conducted in accordance with the local legislation and institutional requirements. The participants provided their written informed consent to participate in this study. The animal

study was approved by the Institutional Animal Care and Use Committee (IACUC), Emory University, Atlanta, GA. The study was conducted in accordance with the local legislation and institutional requirements.

Author contributions

GB: Conceptualization, Data curation, Formal Analysis, Funding acquisition, Investigation, Methodology, Visualization, Writing – original draft, Writing – review & editing. JL: Investigation, Writing – review & editing. JO: Investigation, Writing – review & editing. KP: Investigation, Writing – review & editing. JA: Investigation, Writing – review & editing. RA: Investigation, Writing – review & editing. AF: Resources, Writing – review & editing. BY: Resources, Writing – review & editing. DM: Resources, Writing – review & editing. HB: Resources, Writing – review & editing. SC: Conceptualization, Methodology, Writing – review & editing. BP: Conceptualization, Methodology, Writing – review & editing. CD: Conceptualization, Data curation, Formal Analysis, Funding acquisition, Methodology, Supervision, Writing – review & editing. HS: Conceptualization, Data curation, Formal Analysis, Funding acquisition, Methodology, Supervision, Writing – review & editing.

Funding

The author(s) declare financial support was received for the research, authorship, and/or publication of this article. This work was supported by grants from Curing Kids Cancer and the National Institutes of Health under an R21 grant (5R21CA223300 to HS) and an F31 grant awarded to Emory University (5F31CA265249-02 to GB).

Acknowledgments

The NOMO-1, Kasumi-1, KG-1, and MOLM-13 cell lines were generously donated by the laboratory of Dr. Douglas Graham at Emory University. The CMK cell line was kindly gifted by the laboratory of Dr. Brian Petrich when he was at Emory University. All healthy donor blood samples were obtained through the Emory Children's Clinical and Translational Discovery Core (CCTDC). Flow cytometers were maintained by the Pediatrics/Winship Flow Cytometry Core of Winship Cancer Institute of Emory University, who is supported by Children's Healthcare of Atlanta, Winship Cancer Institute, Emory University and NIH/NCI under award number P30CA138292. All figures were created using BioRender.com.

Conflict of interest

BY, HB, DM, and BP are employees of Expression Therapeutics, which develops cancer immunotherapies using

engineered $\gamma\delta$ T cells. GB, CD, and HS are inventors on a patent application describing ligand-based cell and gene therapies for hematopoietic cancers owned by Emory University and licensed to Expression Therapeutics, Inc. HS and CD are cofounders of Expression Therapeutics and own equity in the company. The terms of these arrangements have been reviewed and approved by Emory University in accordance with its conflict-of-interest policies.

The remaining authors declare that the research was conducted in the absence of any commercial or financial relationships that could be construed as a potential conflict of interest.

The author(s) declared that they were an editorial board member of Frontiers, at the time of submission. This had no impact on the peer review process and the final decision.

References

- Maude SL, Frey N, Shaw PA, Aplenc R, Barrett DM, Bunin NJ, et al. Chimeric antigen receptor T cells for sustained remissions in leukemia. *New Engl J Med* (2014) 371(16):1507–17. doi: 10.1056/NEJMoa1407222
- Davila ML, Riviere I, Wang X, Bartido S, Park J, Curran K, et al. Efficacy and toxicity management of 19-28z Car T cell therapy in B cell acute lymphoblastic leukemia. *Sci Trans Med* (2014) 6(224):224ra25–ra25. doi: 10.1126/scitranslmed.3008226
- Turtle CJ, Hanafi LA, Berger C, Gooley TA, Cherian S, Hudecek M, et al. Cd19 Car-T cells of defined Cd4+:Cd8+ Composition in adult B cell all patients. *J Clin Invest* (2016) 126(6):2123–38. doi: 10.1172/jci85309
- Abramson JS, Palomba ML, Gordon LI, Lunning MA, Wang M, Arnason J, et al. Lisocabtagene maraleucel for patients with relapsed or refractory large B-cell lymphomas (Transcend nhl 001): A multicentre seamless design study. *Lancet* (2020) 396(10254):839–52. doi: 10.1016/s0140-6736(20)31366-0
- Munshi NC, Anderson LD, Shah N, Madduri D, Berdeja J, Lonial S, et al. Idecabtagene vicleucel in relapsed and refractory multiple myeloma. *New Engl J Med* (2021) 384(8):705–16. doi: 10.1056/nejmoa2024850
- Wang M, Munoz J, Goy A, Locke FL, Jacobson CA, Hill BT, et al. Kte-X19 car T-cell therapy in relapsed or refractory mantle-cell lymphoma. *New Engl J Med* (2020) 382(14):1331–42. doi: 10.1056/nejmoa1914347
- Lichtman MA. A historical perspective on the development of the cytarabine (7 days) and daunorubicin (3 days) treatment regimen for acute myelogenous leukemia: 2013 the 40th anniversary of 7 + 3. *Blood Cells Mol Dis* (2013) 50(2):119–30. doi: 10.1016/j.bcmd.2012.10.005
- Briot T, Roger E, Thépot S, Lagarce F. Advances in treatment formulations for acute myeloid leukemia. *Drug Discovery Today* (2018) 23(12):1936–49. doi: 10.1016/j.drudis.2018.05.040
- Rubnitz JE, Razzouk BI, Lensing S, Pounds S, Pui CH, Ribeiro RC. Prognostic factors and outcome of recurrence in childhood acute myeloid leukemia. *Cancer* (2007) 109(1):157–63. doi: 10.1002/cncr.22385
- de Rooij JD, Zwaan CM, van den Heuvel-Eibrink M. Pediatric Aml: from biology to clinical management. *J Clin Med* (2015) 4(1):127–49. doi: 10.3390/jcm4010127
- Lie SO, Abrahamsson J, Clausen N, Forestier E, Hasle H, Hovi L, et al. Long-term results in children with Aml: Nopho-Aml study group—report of three consecutive trials. *Leukemia* (2005) 19(12):2090–100. doi: 10.1038/sj.leu.2403962
- Smith FO, Alonzo TA, Gerbing RB, Woods WG, Arceci RJ, Children's Cancer G. Long-term results of children with acute myeloid leukemia: A report of three consecutive phase iii trials by the children's cancer group: Ccg 251, Ccg 213 and Ccg 2891. *Leukemia* (2005) 19(12):2054–62. doi: 10.1038/sj.leu.2403925
- Sander A, Zimmermann M, Dworzak M, Fleischhack G, von Neuhoff C, Reinhardt D, et al. Consequent and intensified relapse therapy improved survival in pediatric Aml: results of relapse treatment in 379 patients of three consecutive Aml-Bfm trials. *Leukemia* (2010) 24(8):1422–8. doi: 10.1038/leu.2010.127
- Kim MY, Yu K-R, Kenderian SS, Ruella M, Chen S, Shin T-H, et al. Genetic inactivation of Cd33 in hematopoietic stem cells to enable car T cell immunotherapy for acute myeloid leukemia. *Cell* (2018) 173(6):1439–53.e19. doi: 10.1016/j.cell.2018.05.013
- Heo SK, Noh EK, Kim JY, Jeong YK, Jo JC, Choi Y, et al. Targeting C-kit (Cd117) by dasatinib and radotinib promotes acute myeloid leukemia cell death. *Sci Rep* (2017) 7(1):15278. doi: 10.1038/s41598-017-15492-5
- Hassan HT. C-kit expression in human normal and Malignant stem cells prognostic and therapeutic implications. *Leuk Res* (2009) 33(1):5–10. doi: 10.1016/j.leukres.2008.06.011
- Russell AL, Prince C, Lundgren TS, Knight KA, Denning G, Alexander JS, et al. Non-genotoxic conditioning facilitates hematopoietic stem cell gene therapy for hemophilia a using bioengineered factor viii. *Mol Ther Methods Clin Dev* (2021) 21:710–27. doi: 10.1016/j.omtm.2021.04.016
- Czechowicz A, Palchaudhuri R, Scheck A, Hu Y, Hoggatt J, Saez B, et al. Selective hematopoietic stem cell ablation using cd117-antibody-drug-conjugates enables safe and effective transplantation with immunity preservation. *Nat Commun* (2019) 10(1):1–12. doi: 10.1038/s41467-018-08201-x
- Czechowicz A, Kraft D, Weissman IL, Bhattacharya D. Efficient transplantation via antibody-based clearance of hematopoietic stem cell niches. *Science* (2007) 318(5854):1296–9. doi: 10.1126/science.1149726
- Palchaudhuri R, Saez B, Hoggatt J, Schajnovitz A, Sykes DB, Tate TA, et al. Non-genotoxic conditioning for hematopoietic stem cell transplantation using a hematopoietic-cell-specific internalizing immunotoxin. *Nat Biotechnol* (2016) 34(7):738–45. doi: 10.1038/nbt.3584
- Arai Y, Choi U, Corsino CI, Koontz SM, Tajima M, Sweeney CL, et al. Myeloid conditioning with C-kit-targeted car-T cells enables donor stem cell engraftment. *Mol Ther* (2018) 26(5):1181–97. doi: 10.1016/j.ymthe.2018.03.003
- Myburgh R, Kiefer JD, Russkamp NF, Magnani CF, Nuñez N, Simonis A, et al. Anti-human Cd117 car T-cells efficiently eliminate healthy and Malignant Cd117-expressing hematopoietic cells. *Leukemia* (2020) 34(10):2688–703. doi: 10.1038/s41375-020-0818-9
- Muffy LS, Chin M, Kwon H-S, Lieber C, Smith S, Sikorski R, et al. Early results of phase I study of Jsp191, an anti-Cd117 monoclonal antibody, with non-myeloablative conditioning in older adults with Mrd-positive Mds/Aml undergoing allogeneic hematopoietic cell transplantation. *J Clin Oncol* (2021) 39(15_suppl):7035. doi: 10.1200/JCO.2021.39.15_suppl.7035
- Jasper Therapeutics I. *Jasper Therapeutics to Present New Positive Data on Briquilimab Conditioning in Patients with Fanconi Anemia at the 2023 Fanconi Anemia Research Fund Scientific Symposium [Press Release]*. Available at: <https://ir.jaspertherapeutics.com/news-releases/news-release-details/jasper-therapeutics-present-new-positive-data-briquilimab>.
- Gill S, Maus MV, Porter DL. Chimeric antigen receptor T cell therapy: 25years in the making. *Blood Rev* (2016) 30(3):157–67. doi: 10.1016/j.blre.2015.10.003
- Long AH, Haso WM, Shern JF, Wanhainen KM, Murgai M, Ingaramo M, et al. 4-1bb costimulation ameliorates T cell exhaustion induced by tonic signaling of chimeric antigen receptors. *Nat Med* (2015) 21(6):581–90. doi: 10.1038/nm.3838
- Zajc CU, Salzer B, Taft JM, Reddy ST, Lehner M, Traxlmayr MW. Driving cars with alternative navigation tools – the potential of engineered binding scaffolds. *FEBS J* (2021) 288(7):2103–18. doi: 10.1111/febs.15253
- Butler SE, Brog RA, Chang CH, Sentman CL, Huang YH, Ackerman ME. Engineering a natural ligand-based car: directed evolution of the stress-receptor Nkp30. *Cancer Immunol Immunother* (2021) 71:165–76. doi: 10.1007/s00262-021-02971-y
- Pistoia V, Tumino N, Vacca P, Veneziani I, Moretta A, Locatelli F, et al. Human $\Gamma\delta$ T-cells: from surface receptors to the therapy of high-risk leukemias. *Front Immunol* (2018) 9:984. doi: 10.3389/fimmu.2018.00984
- Blazar BR, Hill GR, Murphy WJ. Dissecting the biology of allogeneic HscT to enhance the Gvt effect whilst minimizing Gvhd. *Nat Rev Clin Oncol* (2020) 17:475–92. doi: 10.1038/s41571-020-0356-4
- Story JY, Zoine JT, Burnham RE, Hamilton JAG, Spencer HT, Doering CB, et al. Bortezomib enhances cytotoxicity of ex vivo-expanded gamma delta T cells against

Publisher's note

All claims expressed in this article are solely those of the authors and do not necessarily represent those of their affiliated organizations, or those of the publisher, the editors and the reviewers. Any product that may be evaluated in this article, or claim that may be made by its manufacturer, is not guaranteed or endorsed by the publisher.

Supplementary material

The Supplementary Material for this article can be found online at: <https://www.frontiersin.org/articles/10.3389/fimmu.2023.1294555/full#supplementary-material>

- acute myeloid leukemia and T-cell acute lymphoblastic leukemia. *Cytotherapy* (2021) 23(1):12–24. doi: 10.1016/j.jcyt.2020.09.010
32. Zoine JT, Knight KA, Fleischer LC, Sutton KS, Goldsmith KC, Doering CB, et al. Ex vivo expanded patient-derived gamma delta T-cell immunotherapy enhances neuroblastoma tumor regression in a murine model. *Oncoimmunology* (2019) 8(8):1593804. doi: 10.1080/2162402X.2019.1593804
33. Sutton KS, Dasgupta A, McCarty D, Doering CB, Spencer HT. Bioengineering and serum free expansion of blood-derived $\Gamma\delta$ T cells. *Cytotherapy* (2016) 18(7):881–92. doi: 10.1016/j.jcyt.2016.04.001
34. Burnham RE, Tope D, Branella G, Williams E, Doering CB, Spencer HT. Human serum albumin and chromatin condensation rescue ex vivo expanded $\Gamma\delta$ T cells from the effects of cryopreservation. *Cryobiology* (2021) 99:78–87. doi: 10.1016/j.cryobiol.2021.01.011
35. Burnham RE, Zoine JT, Story JY, Garimalla SN, Gibson G, Rae A, et al. Characterization of donor variability for $\Gamma\delta$ T cell ex vivo expansion and development of an allogeneic $\Gamma\delta$ T cell immunotherapy. *Front Med* (2020) 7:588453. doi: 10.3389/fmed.2020.588453
36. Fleischer LC, Becker SA, Ryan RE, Fedanov A, Doering CB, Spencer HT. Non-signaling chimeric antigen receptors enhance antigen-directed killing by $\Gamma\delta$ T cells in contrast to $\alpha\beta$ T cells. *Mol Ther Oncol* (2020) 18:149–60. doi: 10.1016/j.jomto.2020.06.003
37. Boucher JC, Yu B, Li G, Shrestha B, Sallman D, Landin AM, et al. Large scale ex vivo expansion of $\Gamma\delta$ T cells using artificial antigen-presenting cells. *J Immunother (Hagerstown Md: 1997)* (2023) 46(1):5. doi: 10.1097/CJI.0000000000000445
38. Jonus HC, Burnham RE, Ho A, Pilgrim AA, Shim J, Doering CB, et al. Dissecting the cellular components of $\Gamma\delta$ T cell expansions to optimize selection of potent cell therapy donors for neuroblastoma immunotherapy trials. *Oncoimmunology* (2022) 11(1). doi: 10.1080/2162402X.2022.2057012
39. Becker SA, Petrich BG, Yu B, Knight KA, Brown HC, Raikar SS, et al. Enhancing the effectiveness of $\Gamma\delta$ T cells by mrna transfection of chimeric antigen receptors or bispecific T cell engagers. *Mol Ther Oncol* (2023) 29:145–57. doi: 10.1016/j.jomto.2023.05.007
40. McLeod C, Gout AM, Zhou X, Thrasher A, Rahbarinia D, Brady SW, et al. St. Jude cloud: A pediatric cancer genomic data-sharing ecosystem. *Cancer Discovery* (2021) 11(5):1082–99. doi: 10.1158/2159-8290.CD-20-1230
41. Zhou X, Edmonson MN, Wilkinson MR, Patel A, Wu G, Liu Y, et al. Exploring genomic alteration in pediatric cancer using proteinpaint. *Nat Genet* (2016) 48(1):4–6. doi: 10.1038/ng.3466
42. Uhlén M, Fagerberg L, Hallström BM, Lindskog C, Oksvold P, Mardinoglu A, et al. Proteomics. Tissue-based map of the human proteome. *Science* (2015) 347(6220):1260419. doi: 10.1126/science.1260419
43. Consortium TU. Uniprot: the universal protein knowledgebase in 2023. *Nucleic Acids Res* (2022) 51(D1):D523–D31. doi: 10.1093/nar/gkac1052
44. Raikar SS, Fleischer LC, Moot R, Fedanov A, Paik NY, Knight KA, et al. Development of chimeric antigen receptors targeting T-cell malignancies using two structurally different anti-Cd5 antigen binding domains in Nk and Crispr-edited T cell lines. *Oncoimmunology* (2018) 7(3):e1407898. doi: 10.1080/2162402X.2017.1407898
45. Zoine JT, Prince C, Story JY, Branella GM, Lytle AM, Fedanov A, et al. Thrombopoietin-based car-T cells demonstrate in vitro and in vivo cytotoxicity to Mpl positive acute myelogenous leukemia and hematopoietic stem cells. *Gene Ther* (2021) 29:1–12. doi: 10.1038/s41434-021-00283-5
46. Lee JY, Jonus HC, Sadanand A, Branella GM, Maximov V, Suttapitugsakul S, et al. Identification and targeting of protein tyrosine kinase 7 (Ptk7) as an immunotherapy candidate for neuroblastoma. *Cell Rep Med* (2023) 4(6):101091. doi: 10.1016/j.xcrm.2023.101091
47. Smith KA, Zsebo KM. Measurement of human and murine stem cell factor (C-kit ligand). *Curr Protoc Immunol* (1992) 4(1):6.17.1–6.17.11. doi: 10.1002/0471142735.im0617s04
48. Lennartsson J, Rönstrand L. Stem cell factor receptor/C-kit: from basic science to clinical implications. *Physiol Rev* (2012) 92(4):1619–49. doi: 10.1152/physrev.00046.2011
49. Rigau M, Ostrouska S, Fulford TS, Johnson DN, Woods K, Ruan Z, et al. Butyrophilin 2a1 is essential for phosphoantigen reactivity by $\Gamma\delta$ T cells. *Science* (2020) 367(6478):eaay5516. doi: 10.1126/science.aay5516
50. Wrobel P, Shojaei H, Schittek B, Gieseler F, Wollenberg B, Kalthoff H, et al. Lysis of a broad range of epithelial tumour cells by human $\Gamma\delta$ T cells: involvement of Nkg2d ligands and T-cell receptor- versus Nkg2d-dependent recognition. *Scand J Immunol* (2007) 66(2-3):320–8. doi: 10.1111/j.1365-3083.2007.01963.x
51. Brenner S, Whiting-Theobald N, Kawai T, Linton GF, Rudikoff AG, Choi U, et al. Cxcr4-transgene expression significantly improves marrow engraftment of cultured hematopoietic stem cells. *Stem Cells* (2004) 22(7):1128–33. doi: 10.1634/stemcells.2003-0196
52. Gill S, Tasian SK, Ruella M, Shestova O, Li Y, Porter DL, et al. Preclinical targeting of human acute myeloid leukemia and myeloablation using chimeric antigen receptor-modified T cells. *Blood* (2014) 123(15):2343–54. doi: 10.1182/blood-2013-09-529537
53. Mardiros A, Dos Santos C, McDonald T, Brown CE, Wang X, Budde LE, et al. T cells expressing Cd123-specific chimeric antigen receptors exhibit specific cytolytic effector functions and antitumor effects against human acute myeloid leukemia. *Blood J Am Soc Hematol* (2013) 122(18):3138–48. doi: 10.1182/blood-2012-12-474056
54. Sauer T, Parikh K, Sharma S, Omer B, Sedloev D, Chen Q, et al. Cd70-specific car t-cells have potent activity against acute myeloid leukemia (aml) without hsc toxicity. *Blood* (2021) 138(4):318–30. doi: 10.1182/blood.2020008221
55. Magnani CF, Myburgh R, Brunn S, Chambovey M, Ponzo M, Volta L, et al. Anti-cd117 car T cells incorporating a safety switch eradicate human acute myeloid leukemia and hematopoietic stem cells. *Mol Ther Oncol* (2023) 30:56–71. doi: 10.1016/j.jomto.2023.07.003
56. Willuda J, Honegger A, Waibel R, Schubiger PA, Stahel R, Zangemeister-Wittke U, et al. High thermal stability is essential for tumor targeting of antibody fragments: engineering of a humanized anti-epithelial glycoprotein-2 (Epithelial cell adhesion molecule) single-chain Fv fragment. *Cancer Res* (1999) 59(22):5758–67.
57. Tilayov T, Hingaly T, Greenspan Y, Cohen S, Akabayov B, Gazit R, et al. Engineering stem cell factor ligands with different C-kit agonistic potencies. *Molecules* (2020) 25(20):4850. doi: 10.3390/molecules25204850
58. Landry JP, Ke Y, Yu G-L, Zhu XD. Measuring affinity constants of 1450 monoclonal antibodies to peptide targets with a microarray-based label-free assay platform. *J Immunol Methods* (2015) 417:86–96. doi: 10.1016/j.jim.2014.12.011
59. Nicholson RI, Gee JMW, Harper ME. Egrf and cancer prognosis. *Eur J Cancer* (2001) 37:9–15. doi: 10.1016/s0959-8049(01)00231-3
60. Arcangeli S, Rotiroti MC, Bardelli M, Simonelli L, Magnani CF, Biondi A, et al. Balance of anti-Cd123 chimeric antigen receptor binding affinity and density for the targeting of acute myeloid leukemia. *Mol Ther* (2017) 25(8):1933–45. doi: 10.1016/j.jymth.2017.04.017
61. Singh AP, Zheng X, Lin-Schmidt X, Chen W, Carpenter TJ, Zong A, et al. Development of a quantitative relationship between car-affinity, antigen abundance, tumor cell depletion and car-T cell expansion using a multiscale systems Pk-Pd model. *mAbs* (2020) 12(1):1688616. doi: 10.1080/19420862.2019.1688616
62. Branella GM, Spencer HT. Natural receptor- and ligand-based chimeric antigen receptors: strategies using natural ligands and receptors for targeted cell killing. *Cells* (2021) 11(1):21. doi: 10.3390/cells11010021
63. Brown CE, Alizadeh D, Starr R, Weng L, Wagner JR, Naranjo A, et al. Regression of glioblastoma after chimeric antigen receptor T-cell therapy. *New Engl J Med* (2016) 375(26):2561–9. doi: 10.1056/nejmoa1610497
64. Alizadeh D, Wong RA, Gholamin S, Maker M, Aftabzadeh M, Yang X, et al. Ifn γ Is critical for car T cell-mediated myeloid activation and induction of endogenous immunity. *Cancer Discovery* (2021) 11(9):2248–65. doi: 10.1158/2159-8290.cd-20-1661
65. Perko R, Kang G, Sunkara A, Leung W, Thomas PG, Dallas MH. Gamma delta T cell reconstitution is associated with fewer infections and improved event-free survival after hematopoietic stem cell transplantation for pediatric leukemia. *Biol Blood Marrow Transplant* (2015) 21(1):130–6. doi: 10.1016/j.bbmt.2014.09.027
66. Minculescu L, Marquart HV, Ryder LP, Andersen NS, Schjoedt I, Friis LS, et al. Improved overall survival, relapse-free-survival, and less graft-vs.-host-disease in patients with high immune reconstitution of Tcr gamma delta cells 2 months after allogeneic stem cell transplantation. *Front Immunol* (2019) 10:1997. doi: 10.3389/fimmu.2019.01997
67. Gentles AJ, Newman AM, Liu CL, Bratman SV, Feng W, Kim D, et al. The prognostic landscape of genes and infiltrating immune cells across human cancers. *Nat Med* (2015) 21(8):938–45. doi: 10.1038/nm.3909
68. Cummins KD, Frey N, Nelson AM, Schmidt A, Luger S, Isaacs RE, et al. Treating relapsed/refractory (Rr) Aml with biodegradable anti-Cd123 car modified T cells. *Blood* (2017) 130:1359.
69. Chen C-L, Faltusova K, Molik M, Savvulidi F, Chang K-T, Necas E. Low C-kit expression level induced by stem cell factor does not compromise transplantation of hematopoietic stem cells. *Biol Blood Marrow Transplant* (2016) 22(7):1167–72. doi: 10.1016/j.bbmt.2016.03.017
70. Beatson RE, Parente-Pereira AC, Halim L, Cozzetto D, Hull C, Whilding LM, et al. Tgf-B1 potentiates V γ 9 δ 2 T cell adoptive immunotherapy of cancer. *Cell Rep Med* (2021) 2(12). doi: 10.1016/j.xcrm.2021.100473
71. Peters C, Meyer A, Kouakanou L, Feder J, Schriker T, Lettau M, et al. Tgf-B Enhances the cytotoxic activity of V δ 2 T cells. *Oncoimmunology* (2019) 8(1):e1522471. doi: 10.1080/2162402X.2018.1522471